AD-A244 048

AFIT/GA/ENY/91D-8

Analysis of Suborbital Launch Trajectories for Satellite Delivery

THESIS

Mark R. Goodell
Captain, USAF

AFIT/GA/ENY/91D-8

DTIC
ELECTE
JAN 08 1992
S B D

BEST AVAILABLE COPY

92-00066

Approved for public release; distribution unlimited

92 1 2 078

AFIT/GA/ENY/91D-8

Analysis of Suborbital Launch Trajectories for Satellite Delivery

THESIS

Presented to the Faculty of the School of Engineering
of the Air Force Institute of Technology
Air University
In Partial Fulfillment of the
Requirements for the Degree of
Master of Science in Space Operations

Mark R. Goodell, B.S.
Captain, USAF

December, 1991

Approved for public release; distribution unlimited

Acknowledgments

Of the many individuals who assisted with this thesis effort, I would like to thank the members of my thesis committee, Dr. William C. Elrod. Capt. John J. Borsi, and Dr. Wiliam E. Wiesel, for the direction that they provided. Others that provided invaluable assistance include Kevin Langan and Carl Tilmann from Wright Laboratories for their help in learning to use OTIS, along with Capt Bryan and Terry Kasten from the NASP Joint Program Office who assisted in the formulation of this project in the first place.

I would especially like to thank my wife and friend Susan for her support and for my children who put up with the many hours I spent away from home. I also acknowledge my mother who supported me in thought, as she suffered with a terminal illness.

Mark R. Goodell

Accession For
NTIS GRA&I ☒
DTIC TAB ☐
Unannounced ☐
Justification
By
Distribution/
Availability Codes
Dist | Avail and/or Special
A-1

Table of Contents

		Page
Acknowledgments		ii
Table of Contents		iii
List of Figures		v
List of Tables		vii
List of Symbols		viii
Abstract		x
I.	Introduction	1
	1.1 Introductory Discussion	1
	1.2 Suborbital Launch Trajectories	2
	1.3 Research Objectives	4
II.	Literature Review	6
	2.1 Multi-Stage Performance Optimization	6
	2.2 Trajectory Optimization	8
	2.3 Trajectory Optimization Programs	9
III.	Methodology	11
	3.1 Representative Vehicle Design	11
	3.2 OTIS Computer Simulation Analysis	12
	3.3 Energy Analysis Formulation	14
	3.3.1 Baseline Vehicle Performance	17
	3.3.2 Analysis of suborbital trajectories	19

		Page
IV.	OTIS Analysis Results	22
	4.1 Baseline Trajectory Performance	22
	4.2 Suborbital Trajectory Performance	23
	4.3 Time Available for Payload Deployment	26
V.	Energy Analysis Results	29
	5.1 Comparison of Energy Analysis and OTIS results	29
	5.2 Sensitivity Analysis	34
VI.	Conclusions and Recommendations	49
Appendix A.	Representative Vehicle Design	51
Appendix B.	Baseline Trajectory Data	56
Appendix C.	Suborbital Trajectory Data	74
Bibliography		90
Vita		91

List of Figures

Figure		Page
1.	Typical NDV ascent path.	3
2.	Illustration of a suborbital trajectory.	4
3.	Specialty areas related to trajectory ıtion.	6
4.	Comparison of a two stage launch vehicle versus a SSTO vehicle to determine the ideal staging velocity (14:4-5).	7
5.	OTIS input and output data files (17:7).	10
6.	Representative vehicle dimensions (3:44) (7:4).	13
7.	Definition of vehicle masses.	15
8.	Optimized baseline trajectory.	23
9.	Baseline and suborbital trajectories.	24
10.	Baseline and pullup trajectories based on OTIS output.	25
11.	Suborbital trajectories with different time periods for payload deployment.	27
12.	Deployment time available for suborbital trajectories.	28
13.	Energy Analysis showing Payload ratio versus all possible pullup starting conditions.	32
14.	Energy Analysis showing Payload ratio versus realistic pullup starting conditions	33
15.	Comparison of energy analysis to OTIS results.	33
16.	Sensitivity Analysis Launch Vehicle Structural Mass 95,200lbm.	37
17.	Sensitivity Analysis with Launch Vehicle Structural Mass 142,800lbm.	37
18.	Sensitivity Analysis with Launch Vehicle Average Airbreathing Specific Impulse 904sec.	38
19.	Sensitivity Analysis with Launch Vehicle Average Airbreathing Specific Impulse 1356sec.	38
20.	Sensitivity Analysis with Launch Vehicle Rocket Specific Impulse 320sec.	39

Figure		Page
21.	Sensitivity Analysis with Launch Vehicle Rocket Specific Impulse 480sec.	39
22.	Sensitivity Analysis with Booster Engine Specific Impulse 320sec. . .	40
23.	Sensitivity Analysis with Booster Engine Specific Impulse of 480 seconds.	40
24.	Sensitivity Analysis with Booster Engine Structural Mass Ratio .08.	41
25.	Sensitivity Analysis with Booster Engine Structural Mass Ratio .12.	41
26.	Sensitivity Analysis with Baseline Transition Velocity of 17,923ft/sec.	42
27.	Sensitivity Analysis with Baseline Transition Velocity of 25,568ft/sec.	42
28.	Sensitivity Analysis with Target Orbit Altitude of 80nm.	43
29.	Sensitivity Analysis with Target Orbit Altitude of 120nm.	43
30.	Sensitivity Analysis with Average Scramjet Dynamic Pressure of 800psf.	44
31.	Sensitivity Analysis with Average Scramjet Dynamic Pressure of 1200psf.	44
32.	Sensitivity Analysis with Deployment Dynamic Pressure of .4psf. . .	45
33.	Sensitivity Analysis with Deployment Dynamic Pressure of .6psf. . .	45
34.	Low Speed Coefficient of Lift (8:21).	52
35.	High Speed Coefficient of Lift.	53
36.	Zero AOA Coefficient of Drag (8:21).	54
37.	Airbreathing Fuel Specific Impulse (9:1).	54
38.	Rocket Fuel Specific Impulse (8:23-24).	55
39.	Baseline Trajectory Altitude versus Time.	71
40.	Baseline Trajectory Thrust versus Time.	71
41.	Baseline Trajectory Flight Path Angle versus Time.	72
42.	Baseline Trajectory Dynamic Pressure versus Time.	72
43.	Baseline Trajectory Temperature versus Time.	73
44.	Suborbital Trajectory Altitude versus Time.	87
45.	Suborbital Trajectory Thrust versus Time.	87
46.	Suborbital Trajectory Flight Path Angle versus Time.	88
47.	Suborbital Trajectory Dynamic Pressure versus Time.	88
48.	Suborbital Trajectory Temperature versus Time.	89

List of Tables

Table		Page
1.	Energy Analysis Baseline Trajectory Results	30
2.	Energy Analysis Suborbital Trajectory Results.	31
3.	Sensitivity Analysis for Design and Trajectory Parameter Assumptions (20% variations).	35
4.	Baseline Payload Capacity Based on Perturbed Performance Parameters.	36
5.	Design Parameters Listed In Order of Importance with Percent Change in Payload Ratio Resulting from Perturbed Performance Values.	46
6.	Design and Performance Parameters used for Energy Analysis.	51
7.	Vehicle Flight Constraints used with OTIS Simulation	55
8.	Summary of Baseline Trajectory Performance.	56
9.	Summary of Suborbital Trajectory Performance.	75

List of Symbols

English Letters

Symbol	Definition
F	Total Launch Vehicle Thrust (lbf)
G	Universal Gravitational Constant $(3.44 \times 10^{-8} \frac{lb\ ft^2}{slug^2})$
g_o	Sea Level gravitational acceleration $(32.175 \frac{ft}{sec^2})$
H, H_{orbit}	Altitude from surface of earth to point along a flight-path or to target orbit (ft)
h	Nondimensional Altitude $(\frac{H}{H_{orbit}})$
Isp	Fuel Specific Impulse defined as $\frac{F}{\dot{w}}$ (sec)
Isp_{ave}	An adjusted Fuel Specific Impulse (sec)
M	Mass of the Earth $(1.31 \times 10^{25} lbm)$
ml,mp,ms	Launch Vehicle payload, propellant, and structure weight (lbm)
mo,mf	Launch Vehicle initial and final weight (lbm)
$ml_{booster}$, $mo_{booster}$	Booster engine payload and initial weight (lbm)
q	Dynamic Pressure (psf)
R, R_1, R_2	Initial to final vehicle mass ratio for different trajectory locations $(\frac{mo}{mf})$
r, r_1, r_2	Altitude measured from center of the earth for different trajectory locations (ft)
S	Nondimensional Velocity $(\frac{V}{V_{cir}})$
V, V_1, V_2	Velocity at different trajectory locations $(\frac{ft}{sec})$
V_{cir}	Orbital Velocity of circular target orbit $(\frac{ft}{sec})$
$\dot{w}$	Propellant Weight Flow Rate $(\frac{lbf}{sec})$
Z	Atmospheric Scale Height $(22907 ft)$

Greek Letters

Symbol	Definition
μ	Gravitational Parameter defined as G x M (4.6868 x $10^{21}\frac{ft^3}{sec^2}$)
ξ	Orbit Specific Mechanical Energy ($\frac{ft^2}{sec^2}$)
Πl,Πp,Πs	Payload, propellant and structural mass divided by initial vehicle mass
ρ, ρ_o	Air density at point along trajectory, and air density at sea level ($.07649\frac{lbm}{ft^3}$)

Abstract

A computer simulation program was used to analyse performance of suborbital launch trajectories using a hypersonic NASP derived vehicle for satellite deployment. The trajectory investigated for this project involved satellite deployment at suborbital speeds. To deploy a satellite in this manner, a booster motor is used to insert the payload into orbit while the launch vehicle reenters and returns to earth. A simplified energy analysis was also formulated and used to determine the sensitivity of suborbital trajectory performance to specific design parameters. Results show that suborbital launch trajectories can increase the useful payload to orbit capacity over an identical vehicle flying a "typical" ascent where both the launch vehicle and payload are inserted into orbit. The amount of time available for payload deployment from a suborbital trajectory was also investigated with results showing that time periods on the order of ten minutes could be used for payload deployment.

Analysis of Suborbital Launch Trajectories for Satellite Delivery

I. Introduction

1.1 Introductory Discussion

The gravity gradient launch trajectory has become widely accepted for space launches using today's multi-stage rocket vehicles. This is due primarily to structural and aerodynamic characteristics that are inherent in todays multi-stage designs. A gravity gradient trajectory relies on gravity instead of control surfaces to rotate the vehicle velocity vector during the launch ascent and thus produces minimum vehicle bending stress. However, the gravity gradient trajectory is not an efficient one with regard to energy requirements. A more efficient flight path involves flight at a non-zero angle of attack, which would require a hypersonic lifting body design. A hypersonic vehicle of this type, would not have the same structural limitations as do the systems currently in use allowing for more flexible launch ascent trajectories to be used.

Recent interest in hypersonic launch vehicle design is apparent in the establishment of the following projects: 1) The National Aero-Space Plane (NASP), 2) The European Hermes Space Plane, 3) The Personnel Launch System and other lifting vehicles that are designed for increased maneuverability at hypersonic speeds. These projects represent a tendency towards the use of more efficient and flexible launch trajectories in the future. Specifically, future launch platforms are expected to incorporate lifting surfaces and air breathing propulsion technology that will provide improved maneuverability and fuel efficiency to the point where a Single-Stage-To-Orbit (SSTO) vehicle may be practical.

The flight characteristics of a hypersonic SSTO vehicle would allow a variety of different ascent trajectories to be used, based on the mission and size of payload to be delivered into orbit. The purpose of this thesis was to investigate a specific satellite launch trajectory that could be utilized by future lifting body launch platforms.

This thesis presents an initial investigation into the use of suborbital launch trajectories for satellite deployment as a means for increasing the payload to orbit

capacity of hypersonic lifting body launch vehicles. The specific trajectory considered for this project involved a pullup maneuver performed by the launch vehicle prior to satellite deployment, release of the payload with a kick booster at the flight path apogee, and the reentry and landing of the launch vehicle. A detailed description of suborbital launch trajectories is presented below.

1.2 Suborbital Launch Trajectories

In order to understand the information presented in this thesis, it is important for the reader to have a clear image of the flight path being analyzed and how it differs from those typically envisioned for a hypersonic lifting body launch vehicle. This section provides a description of a typical ascent profile that a vehicle such as a NASP Derived Vehicle (NDV) is expected to utilize (While the NASP will provide research capabilities only, an NDV would provide operational characteristics that could benefit from the results of this thesis). A description of a suborbital launch trajectory is then provided comparing it to the typical NDV ascent profile. It is important to point out that no consensus exists in the current literature concerning specifics of a typical ascent trajectory for a hypersonic launch platform. Based on a study presented by Lepsch (10:4-5), the following trajectory was defined as a baseline trajectory to be used for this analysis. Note that for the purpose of this thesis, discussion referring to a typical, standard or baseline trajectory, is considered as a reference to the type of trajectory described below.

Figure 1 depicts a typical NDV launch trajectory. This trajectory can be divided into three segments as explained below:

1. Initial Climb and Acceleration - Powered by liquid hydrogen turbine powered and ramjet engines, the hypersonic vehicle will climb to an approximate altitude of 70,000 feet and accelerate to supersonic speed of about Mach 6.
2. Hypersonic Acceleration - Using Supersonic Combustion Ramjet (SCRAMJET) engines, the vehicle will accelerate in a nearly horizontal flight path to a speed of about Mach 20. Note that the final speed to be attained at the end of this phase is a subject of debate with values in current literature ranging from Mach 8 to Mach 22.
3. Orbit Insertion - Having accelerated as far as practical using air breathing propulsion systems, a transition is made to rocket propulsion which will provide

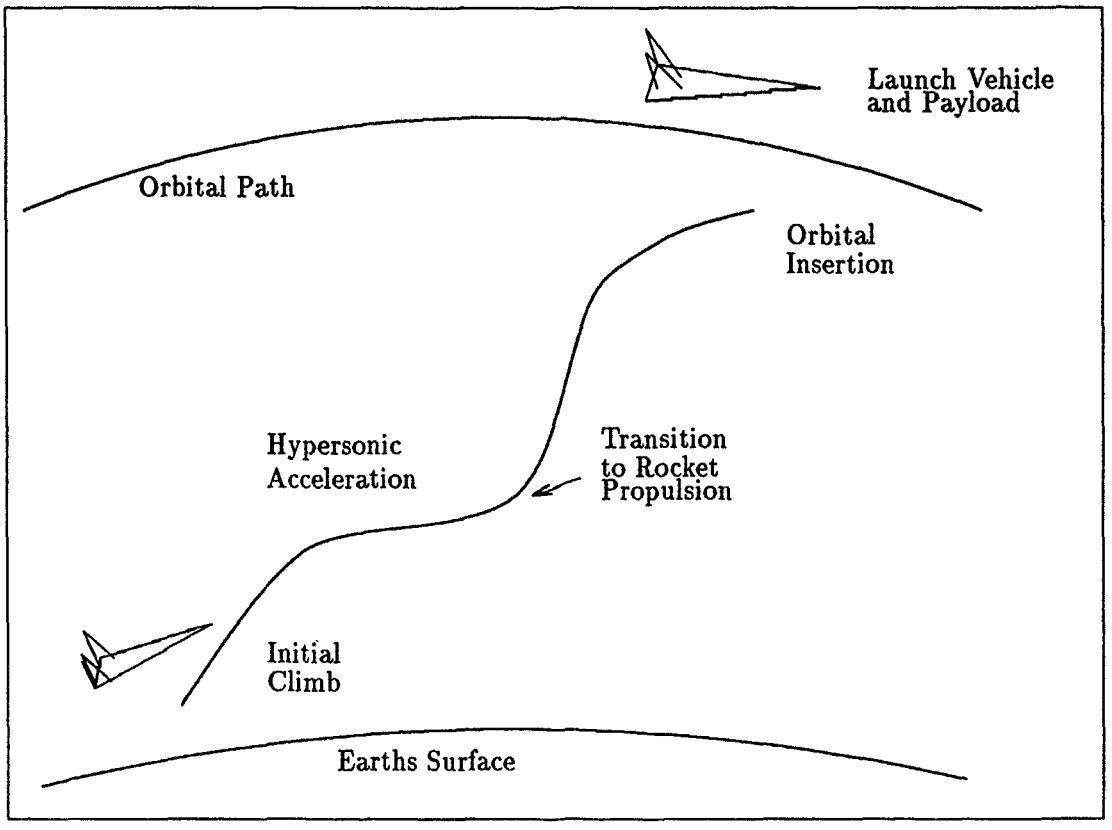

Figure 1. Typical NDV ascent path.

the additional thrust required to place the launch vehicle into a low earth orbit Throughout this thesis, the point at which a launch vehicle transitions from airbreathing to rocket propulsion is referred to as the transition point.

The suborbital launch trajectory analyzed in this document is depicted in Figure 2. This trajectory can also be divided into three separate phases with the first phase identical to that in the previously described trajectory. The second phase is also similar to that of the baseline trajectory except that the speed at which this phase is terminated may be reduced from that of a baseline launch. The main difference with the suborbital trajectory is apparent in the last segment where a pullup maneuver is initiated to transition the launch vehicle flight path from a typical ascent into a suborbital trajectory. Rocket propulsion is then used to raise the launch vehicle to higher altitudes without accelerating the vehicle to the velocity required

to achieve orbit. The payload is separated from the launch vehicle shortly before the flight path apogee. A booster engine attached to the satellite is used to accelerate the payload into the desired orbit while the launch platform falls back into the atmosphere and flies to a landing site. Note that for this project, the research was focused on the ascent portion of suborbital trajectories. No effort was made to analyze the reentry and return to base portions of the launch vehicle flight path.

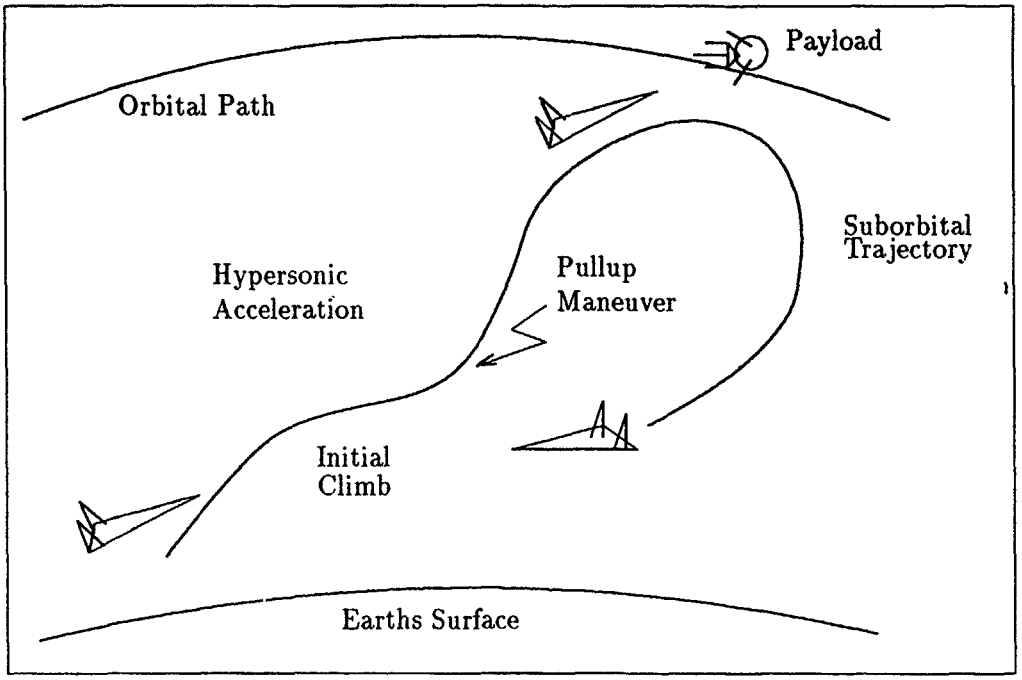

Figure 2. Illustration of a suborbital trajectory.

1.3 Research Objectives

The objectives of this research are listed below:

1. Determine if the use of suborbital trajectories could improve the payload weight to orbit performance of a NDV launch vehicle.
2. Determine the optimal point for the initiation of a pullup maneuver that will maximize the payload weight delivered into orbit.
3. Determine an estimate of the time available for deployment of a payload from a launch vehicle on a suborbital flight path.

4. Determine a first order estimation of the relationship between various launch vehicle design parameters and suborbital launch trajectory performance.

II. Literature Review

Due to the multidisciplinary nature of trajectory analysis as shown in Figure 3, numerous studies were available in current literature that contributed to this research. In particular, studies concerning hypersonic vehicle performance, multistage vehicle trajectory optimization, and numerical trajectory optimization methods, provided insight in the area of launch trajectory analysis. This chapter summarizes a few of the studies directly related to this project.

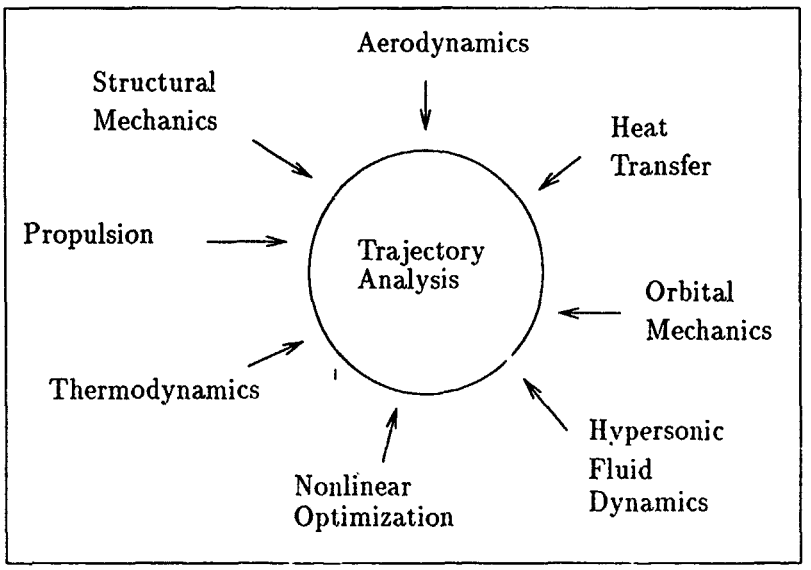

Figure 3. Specialty areas related to trajectory optimization.

2.1 Multi-Stage Performance Optimization

A review of the suborbital trajectories analyzed in this thesis, shows that a suborbital launch ascent is utilizing the concept of staging similar to that used by multi-stage boosters. In the case of a suborbital launch trajectory, the launch vehicle can be considered as the first stage while the payload booster engine serves as the second stage. This similarity between suborbital trajectories and multi-stage boosters allowed for the use of multi-stage performance optimization techniques for this thesis effort.

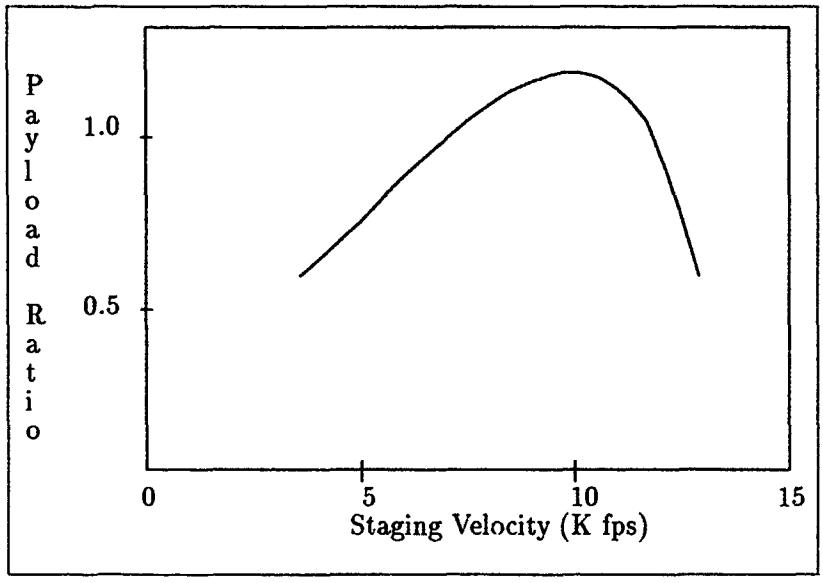

Figure 4. Comparison of a two stage launch vehicle versus a SSTO vehicle to determine the ideal staging velocity (14:4-5).

Several studies have been presented that analyze tradeoffs between one and two stage hypersonic launch vehicle designs (13) (14). Sponable (14:4-5) presents an overview of one and two stage hypersonic launch vehicle designs along with an analysis of various benefits and disadvantages of the different design approaches. While this particular study by Sponable looks mostly into the required technologies for SSTO operations, it also develops a procedure for comparing various one and two stage designs. Part of the study presented by Sponable includes the investigation of the ideal staging velocity for a specific two stage design by comparing the two stage vehicle performance against that of a baseline SSTO design. The results of this study are shown in Figure 4, where payload ratio represents the total payload to orbit capacity of a two stage vehicle design divided by the payload capacity of a baseline single stage design. This same procedure was useful in analyzing sub-orbital launch trajectories as is explained in the next chapter.

The analysis presented in this thesis represents an extension to the study performed by Sponable. One difference that is important to note between these two studies is illustrated by the fact that the study presented by Sponable compared the performance of two separate vehicle designs (SSTO versus a two stage launch vehicle). However, this project compared the performance of only one vehicle type

for two different ascent trajectories. The performance of the two different ascent trajectories was then compared in a manner similar to that used by Sponable so that the impact to the launch vehicle payload capacity could be determined.

2.2 Trajectory Optimization

Many engineering problems require the determination of the optimal solution from a set of all possible solutions. This is the case when comparing space launch trajectories since there is typically an infinite set of trajectories that exist between two points. However, the most desirable of all possible flight paths will typically maximize a certain performance parameter such as propellant consumption or time of flight. According to Vinh (16:1), the analysis of optimal space trajectories has developed into one of the most challenging and fascinating optimization problems of modern times. A simplified definition of an ascent trajectory optimization problem is explained by Vinh as follows:

> In a gravitational field, and with respect to an inertial frame of reference, a space vehicle M, considered as a point mass with mass m, is subject to the ever-present gravitational force $\vec{m}g$, a thrusting force $\vec{T}$ whenever the propulsive system is operating, and, furthermore, to an aerodynamic force $\vec{A}$, to bring it from the initial state, at time t_o, with a position vector $\vec{r_o}$, velocity $\vec{V_o}$ and mass m_o, to the final state $\vec{r_f}$, $\vec{V_f}$ and m_f at the final time t_f such that a certain function of the final state is maximized. In optimal space transfer, this quantity, called the performance index, is generally the final mass. (16:1)

This type of trajectory optimization problem, as explained above, can be solved by analyzing a function that is defined to represent the appropriate type of flightpath. This function can be written in the form of $f(\vec{x}(t), \vec{u}(t))$ where $\vec{x}$ defines the vehicle state and $\vec{u}$ defines the vehicle control settings with respect to time. The feasible set of $\vec{x}(t)$ and $\vec{u}(t)$ is that which defines a trajectory between the given initial and final points while satisfying all problem constraints. Typical trajectory optimization problems will have an infinite number of trajectories in the feasible region. Nonlinear programing techniques can be used to search this region and identify an optimal solution. Studies presented by Hargraves, Ravindran and Gill contain additional information on this topic (5:338-342) (12:487-580) (4:205-260).

2.3 *Trajectory Optimization Programs*

The complex numerical methods and earth models required for trajectory optimization have been incorporated into several different computer programs to facilitate the development of optimized flight paths. One of these programs, used extensively for this project, was *Optimal Trajectories by Implicit Simulation* or OTIS. A brief description of OTIS capabilities is provided below as described by the OTIS User's manual (17:2-6) and the OTIS Applications Manual (11:5-7).

OTIS is a FORTRAN program that optimizes trajectories for a wide variety of aerospace vehicles. OTIS simulates various vehicle trajectories by decomposing the trajectory into a linked sequence of individual stages. In OTIS, the boundaries between stages are selected by the analyst so that the definitions for various flight path boundaries and constraints remain constant for the given phase. Additional considerations for the determination of stage boundaries would include changes in thrust models, sudden mass changes from stage separation, or changes in different aerodynamic lift and drag performance models.

The typical input and output of a trajectory optimization problem using OTIS is illustrated in Figure 5. The two primary inputs required by OTIS are the *Namelist File* and the *Tabular Data File*. The Namelist file contains the basic instructions required to define a specific trajectory problem. This file includes information concerning the trajectory boundary conditions and constraints, the various trajectory stages, and a description of the vehicle being simulated. The tabular data file includes information on the aerodynamics, propulsion, and other user defined functions required for the simulation (17:7).

OTIS produces a variety of output information. The primary output is the *Tabular Output File* which contains trajectory time histories and simple plots of various flight parameters as defined by the user. OTIS also produces data files for the production of detailed plots and various other files that may be used for further analysis of a given trajectory.

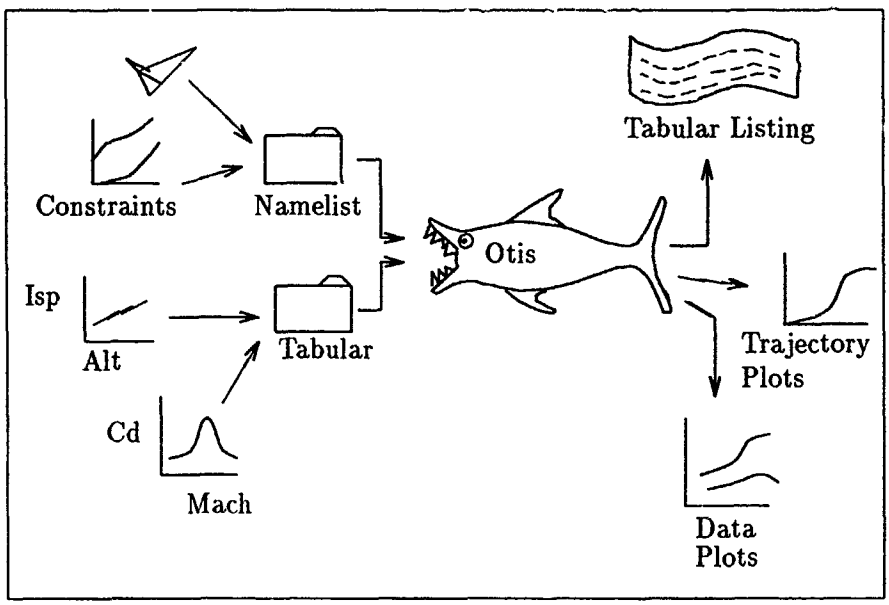

Figure 5. OTIS input and output data files (17:7).

III. Methodology

This thesis presents two different methods for analysis of suborbital launch trajectory performance. The first method utilizes the OTIS simulation program to provide a detailed analysis of several suborbital flight paths. The second method, referred to as an *Energy Analysis*, uses several simplifying assumptions that greatly reduce the complexity of estimating suborbital trajectory performance. The simplified Energy Analysis was used to perform a first order sensitivity analysis of several design assumptions used with the OTIS program. The basic approach of both models was to simulate a baseline trajectory along with several different suborbital trajectories. Relative performance of the suborbital trajectories was then determined through a comparison with the baseline trajectory. In order to simplify the analysis presented in this thesis, the variables used for velocity (V) and altitude (H) where non-dimensionalized as shown in equations 1 and 2 where V_{cir} is final orbital velocity and H_{orbit} is the final orbital altitude.

$$s = \frac{V}{V_{cir}} \tag{1}$$

$$h = \frac{H}{H_{orbit}} \tag{2}$$

While efforts were made in this analysis to provide results that were not dependent on a specific launch vehicle design, it was not possible to produce representative data from general analytic relationships alone. To allow for the desired insight with this project, it was necessary to incorporate physical and aerodynamic models that were representative of launch vehicle performance parameters. The following section explains the vehicle model used in this analysis along with the steps taken to generate data that would provide insight into the relationship between various design assumptions and the overall vehicle performance. The remainder of the chapter then explains the development of the two analytical models used for this project.

3.1 Representative Vehicle Design

Many studies have been performed on hypersonic vehicle performance and stability. Typically these studies also require the use of a representative vehicle design

in order to produce a first approximation of actual hypersonic flight performance. In a study on hypersonic vehicle performance and stability, Drummond presents certain criteria that are important in the selection of a representative vehicle design (3:43). These criteria also apply for this project and are listed below:

1. The vehicle must have the right kind of shape for hypersonic flight.
2. The vehicle must be of sufficient size to perform its envisioned duties.
3. The vehicle must be as simple as possible for ease of analysis (but important features must be accurately accounted for).
4. The vehicle must preferably be similar to shapes for which experimental data is available, so that the results will be as close as possible to true flight behavior.

Based on the above criteria a representative vehicle design was developed as shown in Figure 6. The representative vehicle used in this project was similar to that used by Drummond (3:44-47), however, there are two differences in the overall vehicle design used for this thesis. The differences are: 1) The vehicle in figure 6 was a scaled version with weight fractions similar to those envisioned for a NDV as presented by Kasten (7:4) and 2) Additional aerodynamic characteristics where required to model subsonic and transonic flight regimes for a baseline trajectory. A more detailed description of the representative vehicle used for this project along with aerodynamic and performance characteristics is included in Appendix A.

3.2 OTIS Computer Simulation Analysis

The analytical method presented in this section was used to provide a detailed examination of several suborbital trajectories using the OTIS trajectory simulation program. Advantages of this method included: 1) OTIS generated detailed state information on position, velocity, altitude and numerous other parameters with respect to time for each trajectory that was analyzed, 2) OTIS provided detailed models of the vehicle's aerodynamic and propulsion performance, along with models for aerodynamic heating and the earth's atmosphere and 3) OTIS allowed for the simulation of vehicle performance constraints that influenced the ascent flightpaths. The main disadvantage of this method was the long computer run times required to produce the desired results (approximately three weeks CPU time to optimize a baseline trajectory on a Sparc 2 workstation).

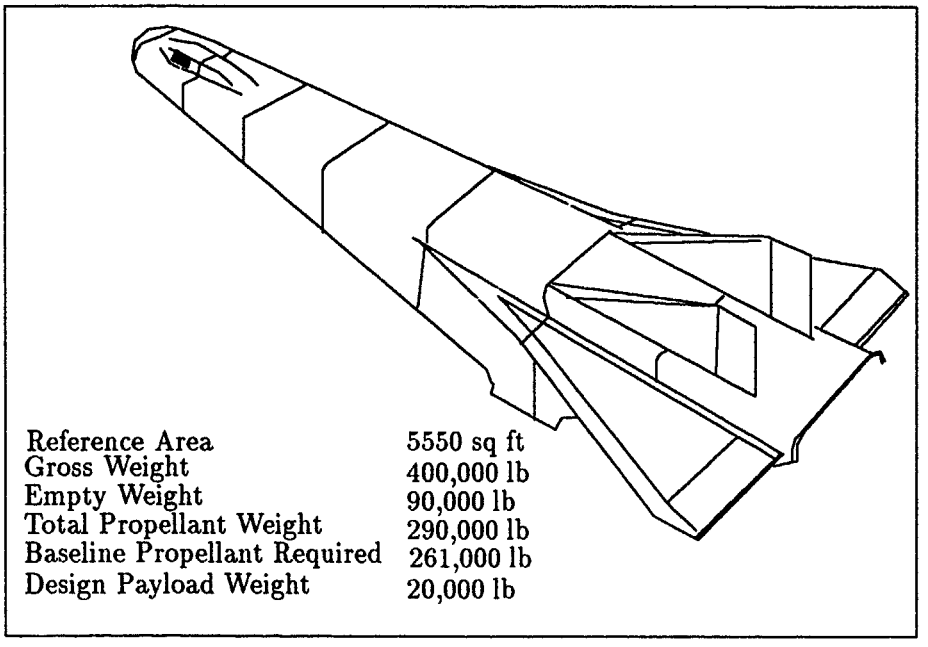

Reference Area	5550 sq ft
Gross Weight	400,000 lb
Empty Weight	90,000 lb
Total Propellant Weight	290,000 lb
Baseline Propellant Required	261,000 lb
Design Payload Weight	20,000 lb

Figure 6. Representative vehicle dimensions (3:44) (7:4).

Along with information on the representative vehicle design, the following conditions were assumed for this analysis:

- The same vehicle design was used for both the analysis of the suborbital and baseline trajectories. The gross takeoff weight was the same regardless of which trajectory was to be simulated.
- Any unused propellant required to fly along a specific suborbital flight path was assumed to be additional payload capacity available for that particular trajectory. Note that the total payload capacity for suborbital trajectories was divided between the kick booster motor and the final payload mass.
- A spherical non-rotating earth was assumed with a 1976 standard atmospheric model used to calculate aerodynamic effects.
- The final payload of both the baseline and suborbital trajectories was delivered to a circular orbit 100nm above the earth surface. This target orbit was used to provide a basis by which the performance of the two different ascent trajectories could be compared.

- Based on OTIS's capability to optimize trajectory performance, no constraint was made concerning the transition point from airbreathing to rocket propulsion along the baseline trajectory. This transition point was identified in the output of the optimized trajectory.
- The only representative vehicle mass values used as inputs for the OTIS trajectory optimization, were the gross and structural weights. The propellant consumption and final payload weight were determined by the OTIS program for each optimized trajectory.

The computer simulation consisted of two separate analysis steps. First an optimal baseline trajectory was identified where both the launch vehicle and the payload were placed into the target orbit. Next, several locations were identified along the baseline trajectory to serve as the starting points for pullup maneuvers leading into different suborbital trajectories. Each suborbital trajectory was then optimized and performance information was calculated. Performance results from the suborbital trajectories were then compared against the baseline trajectory to illustrate the relative performance of the two flight paths.

As mentioned above, the OTIS program calculated propellant consumption and payload weight for each trajectory analyzed. Since simplified aerodynamic and propulsion models were used with the OTIS simulations, it was not expected for the baseline propellant consumption and payload weights to match exactly with those listed for the representative vehicle. Even though simplified models were used in this analysis, the OTIS results were expected to be representative of actual vehicle performance. Comparison of the OTIS mass values to those listed for the representative vehicle was useful in determining how closely the OTIS analysis paralleled the performance expected for the representative vehicle. Note that it was not necessary for the OTIS values to match exactly with those of the representative vehicle since the whole purpose of determining baseline trajectory performance was to provide a basis for comparison of suborbital trajectory performance.

3.3 Energy Analysis Formulation

The analysis presented in this section provided a simplified method for estimating the payload weight that could be placed into orbit using a suborbital launch trajectory. As with the previous section, baseline performance parameters were first

determined for a launch vehicle using a standard ascent trajectory where both the payload and the launch vehicle were placed into the target orbit. Performance parameters were then determined for the same vehicle flying a suborbital ascent trajectory where only the payload was placed into orbit by means of an additional booster motor. The results of these two trajectories were then compared to illustrate the relative performance of the suborbital flight path.

The basis for this analysis consisted of energy and mass fraction definitions as presented by Sutton (15:97) (reference Figure 7), as well as certain performance relationships as shown in equations 3 through 5. In the following equations, V_{cir} is the circular velocity of an orbit at distance r from the center of the earth, ΔV is the total change in velocity required between two points along a trajectory, μ is the universal gravitational constant, ξ is the specific mechanical energy of a given trajectory, and g_o is the sea level gravitational constant.

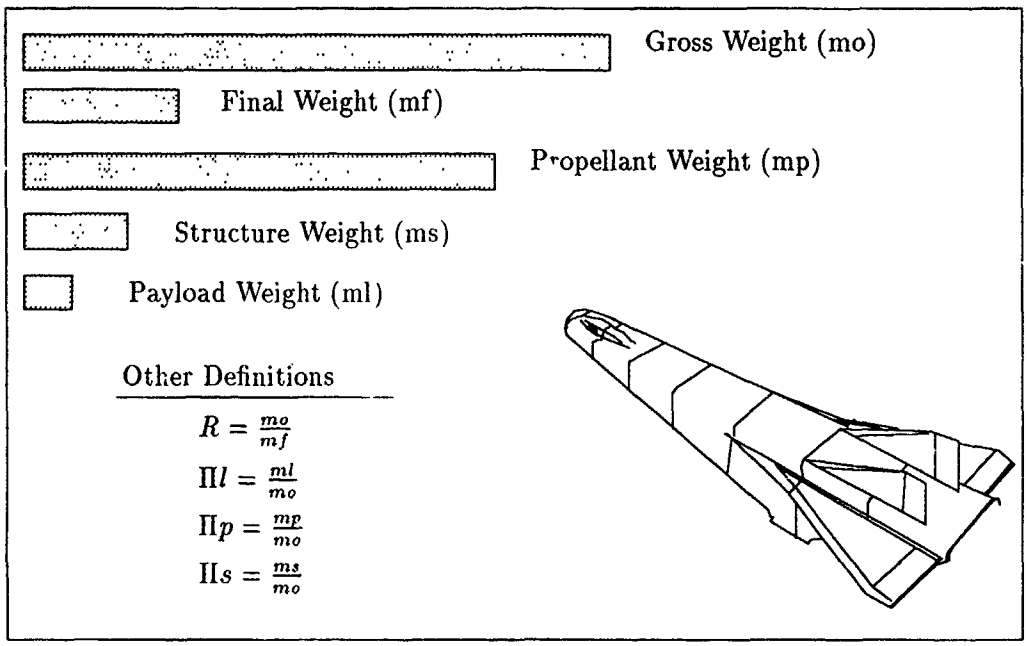

Figure 7. Definition of vehicle masses.

$$V_{cir} = \sqrt{\frac{\mu}{r_{cir}}} \tag{3}$$

$$\xi = \frac{V^2}{2} - \frac{\mu}{r} \tag{4}$$

$$\Delta V = I_{sp}\, g_o \ln R \tag{5}$$

The conditions used for this analysis are listed below. Many of these conditions are similar to those from the OTIS analysis with variations explained in the following list:

- As with the previous subsection, one launch vehicle design was used for both the baseline and suborbital trajectories. It was assumed that the gross takeoff weight for the launch vehicle was the same regardless of which trajectory was to be flown.
- As with the OTIS analysis, any unused propellant required to fly along a suborbital trajectory was assumed to be additional payload capacity.
- For this analysis, a spherical non-rotating earth was assumed, however, atmospheric effects where not considered with this analysis in order to simplify the required calculations.
- As was done with the OTIS analysis, the final payload of both the baseline and suborbital trajectories was delivered to a circular orbit 100nm above the earth surface.
- For the simplified analysis presented here, the transition point had to be assumed for the baseline trajectory. The same transition point velocity identified by OTIS was used with this analysis so that the results of the two different techniques would be based upon the same baseline flight path.
- Use of the energy analysis to calculate baseline trajectory performance, required information concerning the launch vehicle structural, propellant, and payload weights as opposed to OTIS which only required gross and structural weights as inputs. With the OTIS analysis, the propellant and payload weights were calculated by the OTIS program. The same propellant and payload weights that were calculated by OTIS for the baseline trajectory were also used with the energy analysis instead of using the propellant and payload mass values listed for the representative vehicle. Use of the mass values determined by OTIS allowed for a comparison of the two analytical techniques.

3.3.1 Baseline Vehicle Performance As mentioned previously, this analysis was based on certain design and performance characteristics of a representative vehicle as presented in Appendix A. By nature of the vehicle design assumptions, most of the key performance aspects of the baseline trajectory were defined. The analysis of the baseline trajectory was used to calculate launch vehicle performance characteristics that were not already defined by the initial design assumptions. The energy analysis technique was used in two different cases for this analysis where 1) the average airbreathing specific impulse (Isp_{ave}) was estimated and 2) the baseline trajectory payload capacity was estimated using the analysis method explained below. The analysis used for the first case, where the average launch vehicle airbreathing specific impulse was not known, is explained first.

To calculate the required performance information, the baseline ascent was divided into two different segments. These two segments consisted of 1) the airbreathing portion of the ascent and 2) the rocket powered portion of the ascent. The two baseline trajectory segments were divided at the baseline transition point where the launch vehicle propulsion system was switched from airbreathing to rocket propulsion. One of the flight path parameters required to perform the energy analysis was the velocity at which the baseline transition point occurs. Based on the velocity of the baseline transition point, the altitude of the transition point was estimated by applying the dynamic pressure limits as presented in Appendix A. Since both upper and lower dynamic pressure limits exist for the airbreathing portion of the ascent trajectory, an average value of 1000psf was used to estimate the altitude of the baseline transition point. The estimation of the transition point altitude involved the assumption of an exponentially distributed atmosphere as shown in equation 6 where ρ is the air density at altitude H, ρ_o is the air density at sea level and Z is the atmospheric scale height. By combining equation 6 with the dynamic pressure relationship shown in equation 7, the altitude of the baseline transition point could be estimated as shown in equation 8 where q is the dynamic pressure at the transition point.

$$\rho = \rho_o \, e^{\frac{-H}{Z}} \tag{6}$$

$$q = \frac{\rho V^2}{2g_c} \tag{7}$$

$$H = -Z\ Ln\frac{2\ q\ g_c}{\rho_o\ V^2} \tag{8}$$

After a transition point altitude had been calculated, it was necessary to derive a relationship that would approximate the total ΔV required to move between two different points of a trajectory. By assuming an instantaneous propellant burn and that the total specific energy (ξ) immediately following the ΔV is the same as at the second trajectory point, equation 4 was used to develop the relationship shown in equation 9. Equation 9 could then be solved for ΔV to estimate the total velocity change required to move between the two trajectory points as shown in equation 10.

$$\frac{(V_1 + \Delta V)^2}{2} - \frac{\mu}{r_1} = \frac{V_2^2}{2} - \frac{\mu}{r_2} \tag{9}$$

$$\Delta V = \sqrt{2(\frac{V_2^2}{2} - \frac{\mu}{r_2} + \frac{\mu}{r_1})} - V_1 \tag{10}$$

Based on the results of equation 10, it was possible to solve for the amount of propellant consumed along segment 2 of the baseline trajectory. This was done by first calculating the mass ratio R using equation 5 rearranged into the form shown in equation 11. The propellant consumed along segment 2 (mp_2) was then calculated by rearranging the definition for the mass ratio R as shown in equation 12.

$$R = e^{\frac{\Delta V}{Isp\ go}} \tag{11}$$

$$mp_2 = (R_2 - 1)(ml + ms) \tag{12}$$

The next step was to calculate the average specific impulse (Isp_{ave}) along segment 1 in such a manner that all available propellant was consumed along the entire trajectory. First the amount of propellant available for segment 1 was calculated by subtracting the propellant used in segment 2 from the total propellant mass. Next, the vehicle mass ratio R for segment 1, was calculated as shown in equation 13. The ΔV required for segment 1 was calculated using equation 10 which then allowed for the calculation of the average specific impulse by rearranging equation 5 into the form shown in equation 14.

$$R_1 = \frac{mo}{mf_1} = \frac{ms + ml + mp_1 + mp_2}{ms + ml + mp_2} \tag{13}$$

$$Isp_{ave} = \frac{\Delta V_1}{g_o \, Ln \, R_1} \tag{14}$$

There were also cases where the energy analysis was used when the average airbreathing specific impulse (Isp_{ave}) did not need to be calculated, however, the payload capacity of the given trajectory was unknown. In these cases, most of the calculations used to estimate the launch vehicle payload capacity were the same as those used to determine the average airbreathing specific impulse. The ΔV required for each of the trajectory segments was calculated using equation 10 and then the mass ratio for each segment was determined using equation 11. An iterative procedure was then used to solve for the final trajectory payload capacity based on the launch vehicle mass ratio (R) for each flight path segment, and the fact that the launch vehicle gross takeoff weight was a constant (400,000 lbm) for each trajectory analyzed. This iterative procedure required an initial guess of the launch vehicle payload capacity for the case being analyzed. Based on the assumed payload capacity, the propellant consumption for segment 2 could be calculated using equation 12 and for segment 1 using equation 15. Next, a calculated value for the gross launch vehicle weight (mo_{calc}) was determined using equation 16. The estimated gross launch weight was then compared against the actual gross weight of 400,000 lbm. If the two values did not match, then the procedure was repeated with a new estimated for the payload capacity until the calculated gross weight compared favorably with the actual vehicle takeoff weight. This routine resulted in the calculation of the trajectory propellant consumption (the sum of mp_1 and mp_2) and the baseline launch vehicle payload capacity.

$$mp_1 = (R_1 - 1)(ml + ms + mp_2) \tag{15}$$

$$mo_{calc} = ms + ml + mp_1 + mp_2 \tag{16}$$

3.3.2 Analysis of suborbital trajectories The analysis of suborbital trajectories was done in a manner similar to that used for the baseline analysis. For this

case, the suborbital trajectory was divided into three different segments as follows: 1) the airbreathing portion of the trajectory up to the suborbital pullup, the rocket powered portion of the trajectory used to raise the launch vehicle altitude from the pullup altitude to a point where payload deployment could occur, and 3) payload deployment and insertion into orbit using a booster motor connected to the payload. In this case, the same average airbreathing specific impulse (Isp_{ave}) was used in segment 1 as was used for segment 1 of the baseline trajectory. In this manner, all the performance parameters were defined except for the final payload weight that was delivered into orbit using the particular suborbital trajectory.. The payload weight delivered into orbit from a suborbital trajectory was calculated by analyzing each trajectory segment individually as explained in the following paragraphs.

As with the baseline trajectory analysis, the altitude of the trajectory midpoints was calculated based on the dynamic pressure at these locations as shown in equation 8. The altitude of the suborbital pullup maneuver was based on an average dynamic pressure of 1,000 psf. The altitude at which payload deployment occurred was found by using the same velocity as the suborbital pullup and a minimum dynamic pressure of 0.5 psf as presented in Appendix A.

Once the altitudes of the trajectory midpoints had been calculated, the next step was to calculate the propellant consumption of each segment. The amount of propellant used in segments 1 and 2 were first calculated based on the ΔV requirement for each segment using equation 10. The vehicle mass ratio R at the end of each segment was then determined from equation 11 and the propellant consumed was then found for the first two flight path segments using equations 12 and 15. The sum of the propellant consumed in the first two flight path segments represented the total launch vehicle propellant requirement for a particular suborbital trajectory.

Once the launch vehicle propellant requirement for a particular suborbital trajectory was known, then any unused propellant was assumed to represent additional payload capacity. In other words, the combined payload and booster engine weight was found by subtracting the weight of propellant consumed and launch vehicle structural weight from the initial vehicle gross weight as shown in equation 17.

$$mo_{booster} = W_{payload} + W_{booster} = mo - ms - mp_1 - mp_2 \tag{17}$$

The next step of this analysis was to determine the final payload weight that was delivered into the target orbit along trajectory segment 3. This was done by calculating the ΔV requirement for segment 3 from equation 10 and the booster mass ratio $R_{booster}$ from equation 11. The final payload weight was then found using equation 18 where $ml_{booster}$ was the final payload weight, $\Pi s_{booster}$ was the booster structural mass fraction, and $mo_{booster}$ was the initial booster weight from equation 17.

$$ml_{booster} = \frac{mo_{booster}}{R_{booster}} - (\Pi s_{booster})\ (mo_{booster}) \tag{18}$$

Once the suborbital trajectory payload capacity had been calculated, the final step was to compare the suborbital trajectory performance against the baseline performance. This was done by defining a variable that was referred to as the *Payload Ratio*. The payload ratio was simply the suborbital trajectory payload capacity divided by the baseline trajectory payload capacity as shown in equation 19. The payload ratio was useful in this analysis since a value greater than one indicated that the particular suborbital trajectory was capable of delivering a heavier payload to the target orbit than was possible with the baseline trajectory.

$$Payload\ \ Ratio = \frac{ml_{booster}}{ml_{baseline}} \tag{19}$$

IV. OTIS Analysis Results

This chapter presents trajectory performance results that were developed with the OTIS program. The information presented here is divided into three categories: 1) baseline trajectory performance, 2) suborbital trajectory performance, and 3) time available for payload deployment.

4.1 Baseline Trajectory Performance

The first step of the OTIS analysis involved the determination of performance information for a baseline trajectory where both the launch vehicle and the payload were placed into orbit. This analysis was performed based on the representative vehicle design and flight constraints listed in Appendix A. The OTIS program was used to optimize a baseline trajectory that would maximize the payload weight to orbit based on the vehicle design criteria. Figure 8 contains an altitude versus speed plot of the baseline trajectory produced with the OTIS program. A tabular listing of the final baseline trajectory along with plots of certain flight parameters produced by OTIS is included in Appendix B.

Review of the suborbital trajectory data in Appendix B shows that the baseline propellant consumption weight calculated by OTIS differs by 8.4% from that listed for the representative vehicle. The baseline propellant requirement generated by OTIS was 239,102 lbm as compared to 261,000 lbm listed for the representative vehicle. As previously mentioned, it was not necessary for the OTIS model to closely match the representative vehicle performance as far as the propellant consumption and payload weight were concerned. However, the close correlation shown by the two baseline propellant consumption values indicate that the simplified aerodynamic and propulsion models used with OTIS provided good approximations of expected vehicle performance.

Comparison of the baseline payload weight determined by OTIS against that of the representative vehicle shows a difference of 109%, a much larger difference than that found for the propellant consumption values. This large discrepancy between the OTIS and representative vehicle payload weights can be expected as a direct result of the difference in the propellant consumption weights. The OTIS propellant consumption was 21,898 lbm less than that listed for the representative vehicle

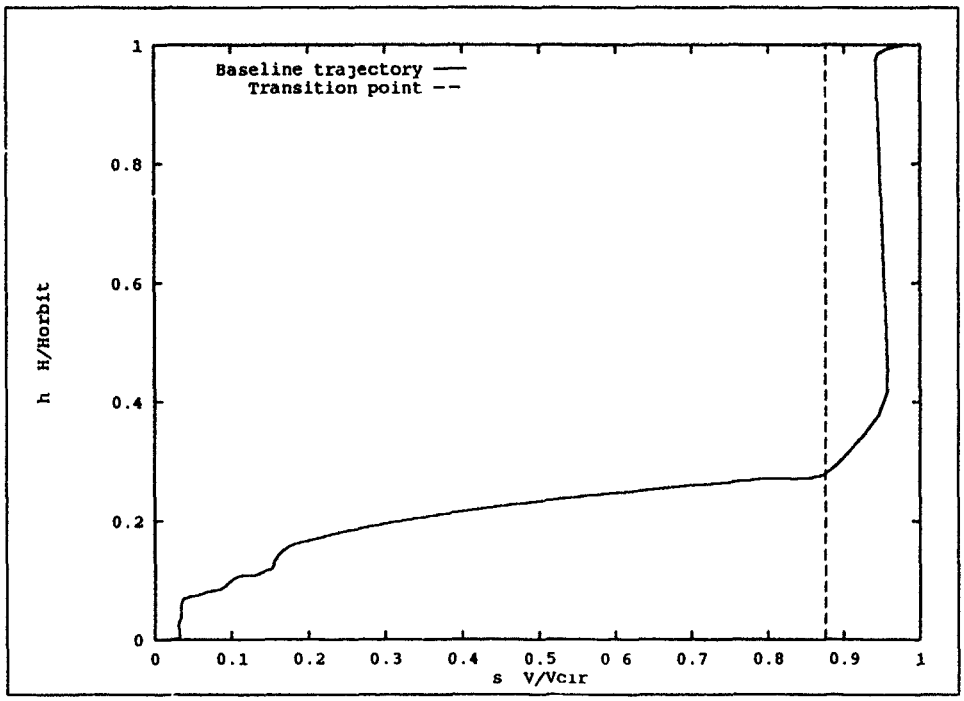

Figure 8. Optimized baseline trajectory.

resulting in an increase in the vehicle payload weight by the same amount (41,898 lbm payload for the OTIS analysis compared to 20,000 lbm for the representative vehicle).

An interesting observation that can be made from the optimized baseline trajectory shown in Figure 8 is the point at which the transition occurs from airbreathing propulsion to rocket propulsion. The transition point was determined by the OTIS program in a manner that would optimize the payload weight delivered into orbit while satisfying the various flight constraints as listed in Appendix A. For this baseline trajectory, the transition point occurs at a speed ratio of .876 and an altitude ratio of .279. These values correspond to a velocity of 22403 ft/sec (Mach 20.7) and an altitude of 169,475 feet. The transition point is indicated in Figure 8 by a vertical dotted line.

4.2 Suborbital Trajectory Performance

After a baseline trajectory had been produced, several points were selected along the baseline flight path as starting conditions for pullup maneuvers that would

lead into several different suborbital trajectories. The points selected for the initiation of pullup maneuvers were selected from both the airbreathing and rocket powered portions of the baseline trajectory. Each individual suborbital launch trajectory was then optimized to deliver the maximum payload to orbit. Figure 9 illustrates a few of the suborbital trajectories analyzed by OTIS as compared to the baseline trajectory. The tabular output from an optimized suborbital analysis is included in Appendix C along with plots of various flight parameters.

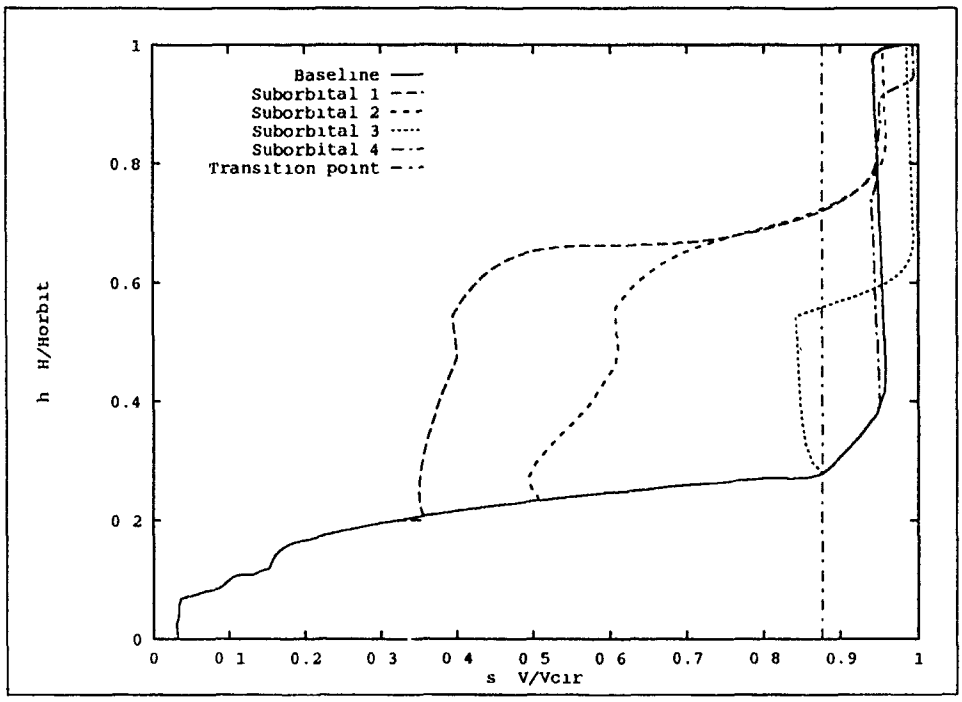

Figure 9. Baseline and suborbital trajectories.

The optimization of each suborbital trajectory resulted in a different payload capacity for each individual flight path. A comparison of the payload capacity for several different suborbital trajectories was made against the payload capacity of the baseline trajectory. This was done by plotting the payload ratio against the initial pullup speed for several different suborbital trajectories as shown in Figure 10.

Several observations can be made based on the information shown in Figure 10. These observations are listed below:

- The results shown in Figure 10 indicate that the use of suborbital trajectories shows potential for increasing the payload to orbit capacity over that possible

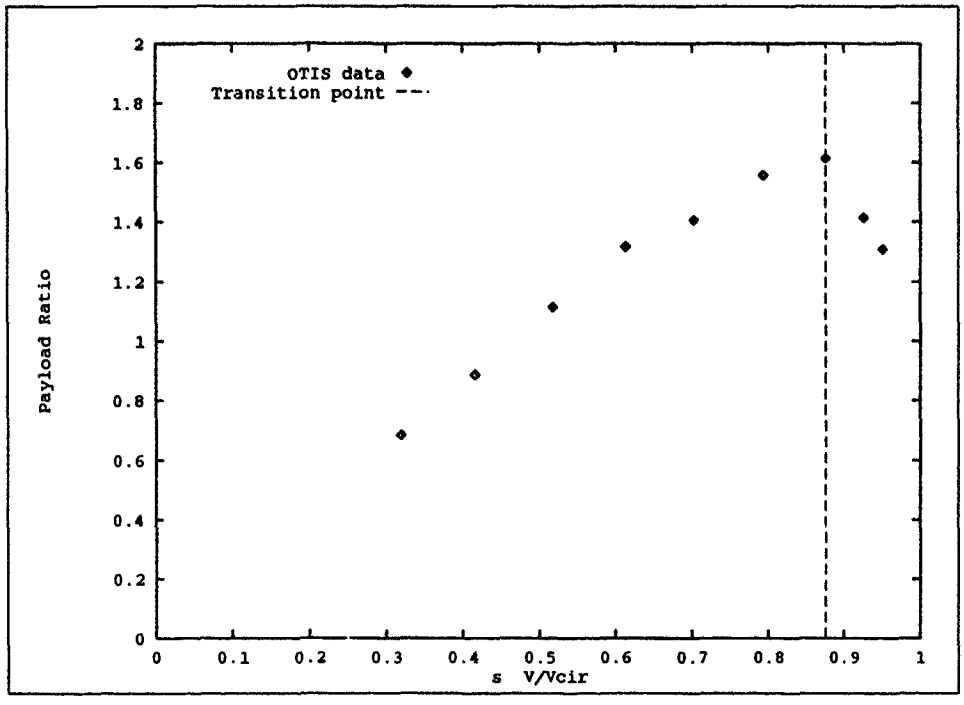

Figure 10. Baseline and pullup trajectories based on OTIS output.

with a normal ascent profile as represented by the baseline trajectory. This observation is based on the portion of Figure 10 where the payload ratio is greater than one.

- Based on this analysis, the best suborbital trajectory performance was achieved when the suborbital trajectory was initiated close to the baseline transition point. This observation has some intuitive support for the following reasons: 1) The best performance trajectory would be expected to take full advantage of the region prior to the transition point due to the higher performance of the airbreathing engines that can be used in this region. The closer the pullup is to the transition point, the less payload acceleration is required by the less efficient rocket engines. 2) For suborbital trajectories initiated after the transition point, the rocket engines are used to accelerate the entire launch vehicle to the pullup velocity. In this region, the suborbital trajectory comes closer and closer to the baseline trajectory as the pullup velocity increases.
- Figure 10 shows a best case suborbital payload capacity that is 61% greater than that of the baseline trajectory. The best case suborbital trajectory (listed

in Appendix C) resulted in a 67,635 lbm payload capacity as compared to the 41,898 lbm payload capacity of the baseline trajectory.

4.3 Time Available for Payload Deployment

Review of the typical baseline ascent trajectory shows that large amounts of time would be available for payload preparation, testing, and deployment. The large time periods result from the fact that the baseline trajectory places the launch vehicle into orbit along with the payload. A suborbital trajectory, however, would be constrained by the amount of time available for satellite deployment based on the limited time spent in a suborbital flight path. For this analysis, satellite deployment is considered to occur during a time period when neither the launch vehicle or payload propulsion systems are used and the external dynamic pressure is less than or equal to the deployment dynamic pressure limit. The OTIS program was used to analyze how the amount of time used for payload deployment effects suborbital trajectory performance.

The suborbital trajectory performance plotted in Figure 10 was based on a payload deployment period of 30 seconds. In order to determine how the deployment period effects trajectory performance, several different suborbital trajectories were analyzed that were initiated from the same initial pullup conditions but with different lengths of time used for satellite deployment. Each trajectory was optimized by the OTIS program to maximize the payload weight to orbit based on the different deployment periods. A few of the resulting trajectories with different deployment times are shown in an altitude versus speed plot in Figure 11.

One observation that can be made from Figure 11 is that suborbital trajectories can be modified in order to accommodate for the amount of time required to deploy a given payload from a launch vehicle. The data used to produce Figure 11 showed that the apogee of the suborbital trajectory followed by the launch vehicle occurred at higher altitudes when longer deployment time periods where used. This pattern can be observed from the first three trajectories plotted in Figure 11 with deployment times of 1, 140, and 200 seconds respectively. The apparent hump in these first three trajectories indicates the separation of the payload from the launch vehicle which coincides with the suborbital trajectory apogee. As shown by the last two trajectories in Figure 11 (deployment times of 320 and 600 seconds), the suborbital trajectory apogee occurred at an altitude higher than that of the target orbit.

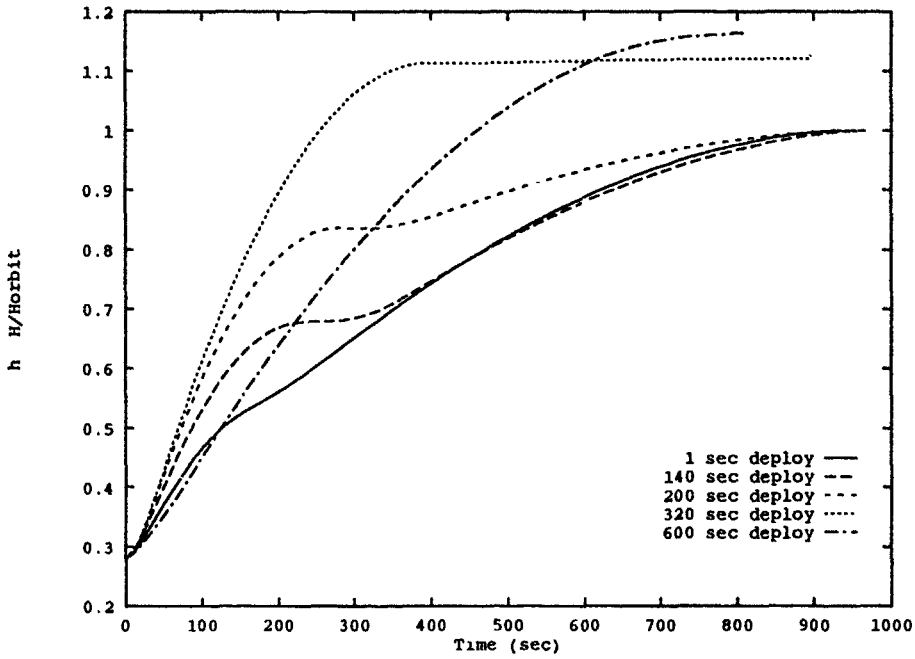

Figure 11. Suborbital trajectories with different time periods for payload deployment.

The effects of various deployment time periods on payload to orbit capacity were determined by plotting the trajectory payload ratio versus the time used for deployment as shown in Figure 12. Figure 12 is useful in illustrating how different deployment time periods effect the payload capacity of suborbital trajectories. This figure shows that for the trajectories analyzed, the payload ratio decreases by up to 28% with deployment periods of up to 700 seconds (The payload ratio is 1.614 with a deployment time of 1.0 seconds compared to a payload ratio of 1.160 with a deployment period of 700 seconds). Suborbital trajectories with deployment periods greater than 700 seconds could not be analyzed for this study due to difficulties caused by the OTIS program.

It should also be noted that for suborbital trajectories with an apogee higher than the target orbit, it would be more efficient to insert the payload into a final orbit that is slightly elliptical. In this case, the payload would be placed into an orbit with a 100 nm perigee and an apogee height the same as that of the suborbital trajectory. For the analysis shown in Figure 12, it was assumed to be acceptable for the payload to be placed into an elliptical orbit with an apogee greater than the target orbit altitude. If the requirement for a circular 100 nm orbit where enforced, the

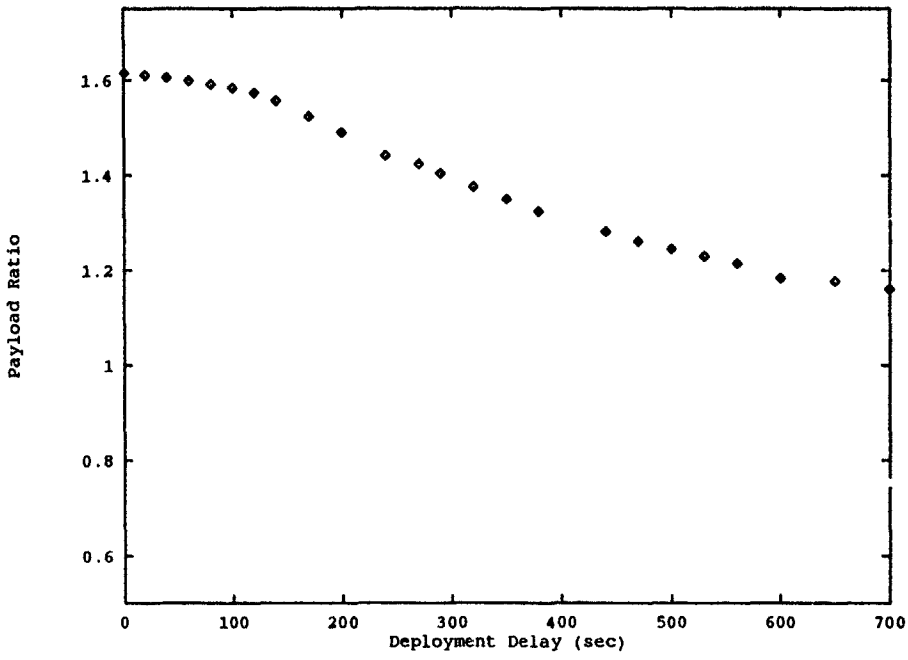

Figure 12. Deployment time available for suborbital trajectories.

performance of trajectories with deployment times greater than about 250 seconds would be decreased from that shown in Figure 12.

V. *Energy Analysis Results*

The results produced using the OTIS program were based on the design parameters and assumptions of the representative vehicle as shown in Appendix A (except for the propellant consumption and payload weights as explained in chapter 3). An analysis of suborbital launch performance based on a different vehicle design would most likely differ from those presented in the previous chapter. The simplified energy analysis technique provided a method for investigating the relationship between the representative vehicle design assumptions and suborbital trajectory performance. This type of analysis could have also been performed using the OTIS computer program but due to the lengthy run times required, the use of OTIS was not practical for this project. The energy analysis results presented in this chapter consist of 1) a comparison of energy analysis results with those generated using OTIS and 2) a sensitivity analysis of vehicle design and flight path assumptions.

5.1 Comparison of Energy Analysis and OTIS results

Use of the energy analysis technique provided a simplified approach for comparing the performance of a suborbital launch trajectory against the performance of a baseline trajectory. Due to the simplifying assumptions of the energy analysis, that do not directly account for atmospheric effects, it was expected that the energy analysis results would differ from those derived using OTIS. This section discusses energy analysis calculations and then makes a comparison of the energy analysis results to those obtained from the OTIS analysis.

The energy analysis was similar to the OTIS analysis in that performance characteristics were first calculated for a baseline trajectory which would then be used for comparison against different suborbital trajectories. Tables 1 and 2 provide some of the results of the energy analysis calculations for the baseline and one suborbital trajectory respectively. The results of interest in these two cases include the average airbreathing specific impulse (Isp_{ave}) in Table 1 and the payload ratio in Table 2. The average airbreathing specific impulse calculated for the baseline trajectory defined the airbreathing engine performance that was then used in the suborbital trajectory analysis. The payload ratio was the final result of the analysis that indicated the

Table 1. Energy Analysis Baseline Trajectory Results

Baseline Trajectory Assumptions	Value	Baseline Analysis Calculations	Value
Payload to orbit	41,898 lbm	Transition Altitude	146,404 ft
Transition Velocity	22403 ft/sec	ΔV segment 1	22,611ft/sec
Orbit Altitude	100 nm	ΔV segment 2	3,718 ft/sec
Dynamic Pressure at Transition Point	1000 psf	R_1 segment 1	1.862
		R_2 segment 2	1.334
		Propellant mass segment 1	185,177 lbm
		Propellant mass segment 2	53,870 lbm
		Isp_{ave} segment 1	1130 sec

relative performance of suborbital trajectories as compared to baseline trajectory performance.

The next step of the energy analysis was to calculate trajectory performance for various suborbital trajectories and compare the results to that of the baseline flight path. Table 2 includes some of the key parameters calculated in the analysis of a particular suborbital trajectory. The result of interest is the payload ratio where the payload capacity of a particular suborbital trajectory is divided by the payload capacity of the baseline ascent trajectory.

Due to the flexibility allowed by the energy analysis, it was possible to determine the relative performance for a wide range of suborbital trajectories with initial pullup velocities ranging from zero to orbital speed and the initial pullup altitude ranging from zero to orbital altitude. The results of an analysis of all possible suborbital trajectories is shown in Figure 13 as a plot of payload ratios versus pullup initial conditions.

While Figure 13 was useful for illustrating the relation of suborbital trajectory performance for various pullup starting conditions, most of the points in this graph were unrealistic for actual application. For example, the extreme pullup starting points of orbital altitude and zero velocity or zero altitude and orbital velocity make little sense as the initial conditions for a suborbital trajectory. It was determined that

Table 2. Energy Analysis Suborbital Trajectory Results.

Suborbital Trajectory Performance Parameter	Value
Popup Velocity	22403.4 ft/sec
Popup Altitude	146,404 ft
ΔV segment 1	22,611 ft/sec
ΔV segment 2	243 ft/sec
ΔV booster	3,514 ft/sec
Propellant burned seg 1	185,177 lbm
Propellant burned seg 2	4,037 lbm
Booster propellant	21,923 lbm
Booster structure	2,192 lbm
Final Payload weight	67,671 lbm
Payload Ratio (Suborbital/Baseline)	1.62

a more realistic set of pullup starting conditions could be obtained by applying the dynamic pressure constraints listed in Appendix A. These dynamic pressure limits require a minimum of 400psi for scramjet operation and a maximum of 2000psi to maintain structural integrity. Application of these dynamic pressure limits are indicated by the narrow dark band in Figure 13. As can be observed in Figure 13, application of the dynamic pressure limits eliminated nearly all of the pullup starting conditions. The remaining points represented a more realistic set of pullup starting conditions that were then plotted as shown in Figure 14.

Since the energy analysis was used to calculate suborbital trajectory performance based on the same vehicle design parameters as used with the OTIS analysis, it is useful to compare the results of the two different analysis techniques. This comparison is shown in Figure 15. The following observations can be made from the information presented in this figure:

- Figure 15 shows a very good correlation between the OTIS and energy analysis results for suborbital trajectories initiated during the airbreathing portion of the baseline ascent. However, the results of the two analysis techniques appear to deviate for trajectories initiated during the rocket powered portion of the

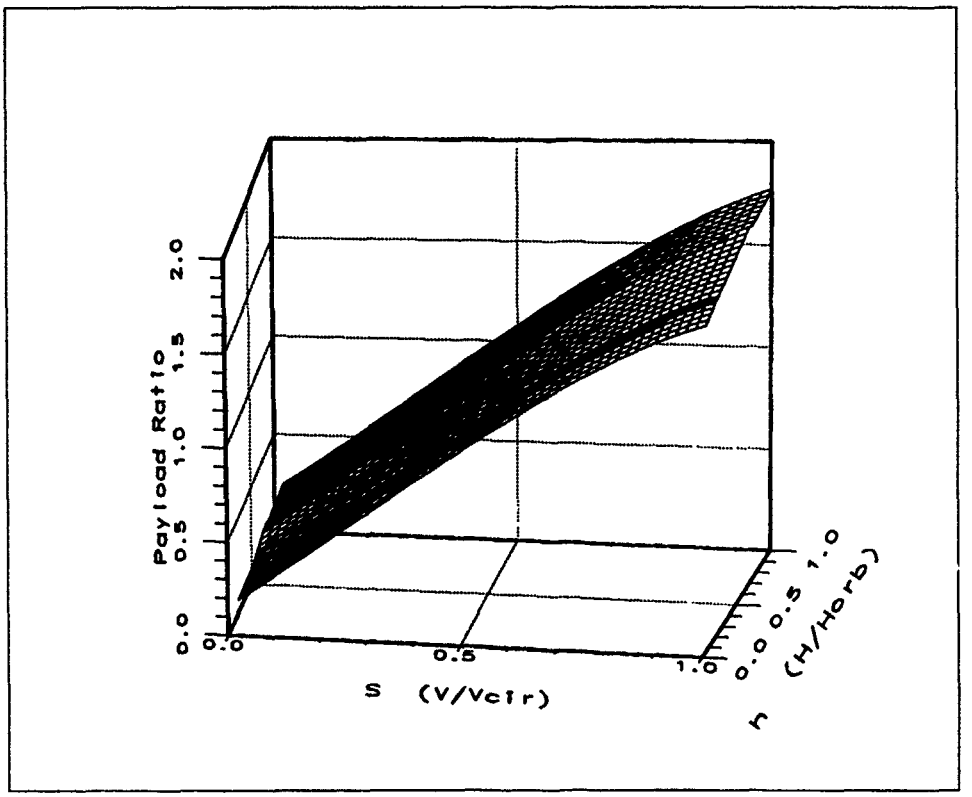

Figure 13. Energy Analysis showing Payload ratio versus all possible pullup starting conditions.

ascent. A closer review of the energy analysis technique helps to explain the deviation. The energy analysis assumed airbreathing propulsion was always used up to the initiation of the pullup maneuver. The OTIS analysis did not allow for airbreathing propulsion at speeds greater than that of the baseline transition point resulting in a more realistic trajectory simulation. Since two different assumptions were used for suborbital trajectories initiated after the baseline transition point, it was expected to observe a deviation between the two analysis methods in this region.

- The good correlation between the OTIS and energy analysis data established a basis for the use of the energy analysis for estimating suborbital trajectory performance.

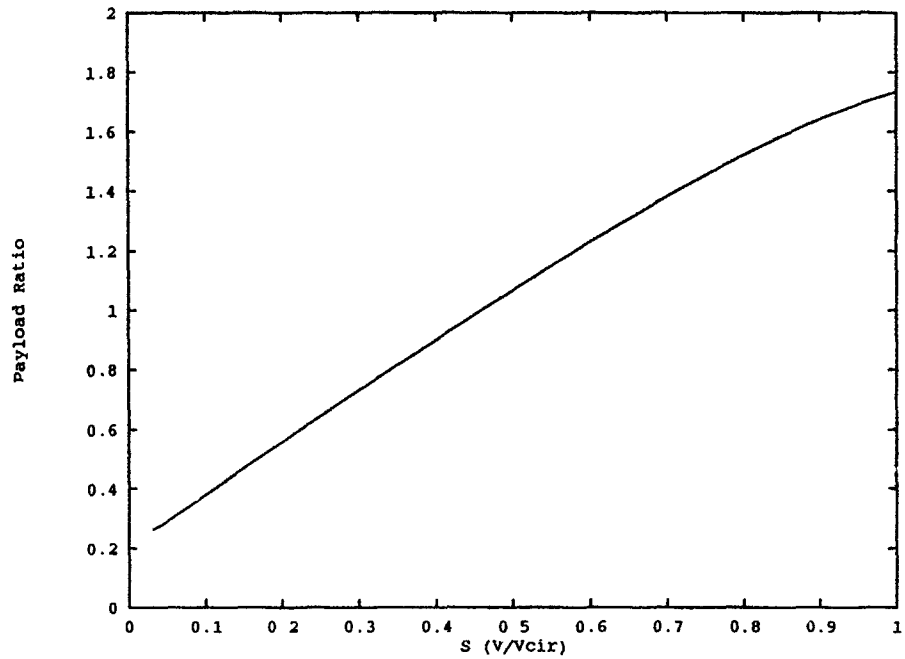

Figure 14. Energy Analysis showing Payload ratio versus realistic pullup starting conditions

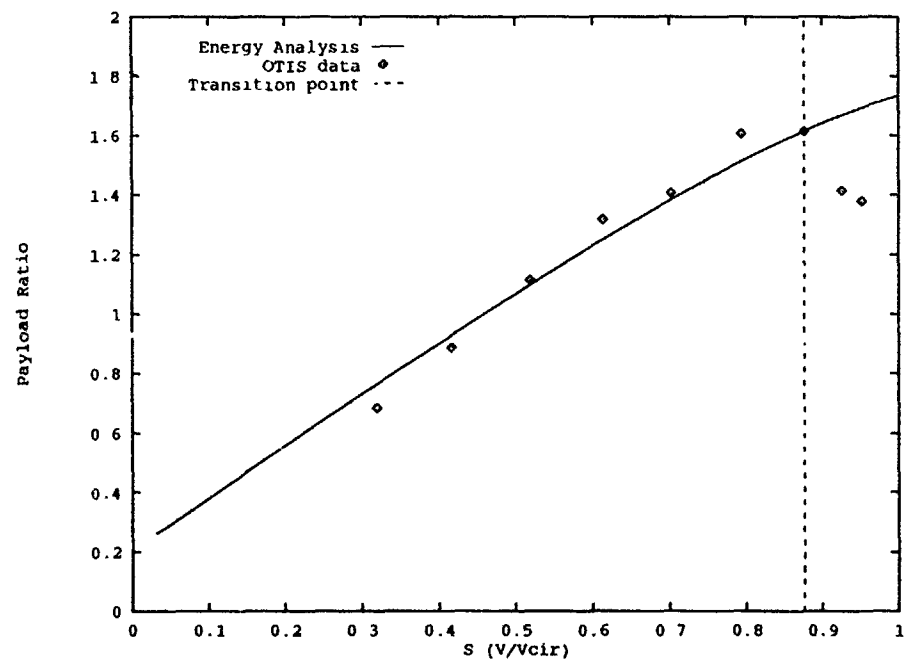

Figure 15. Comparison of energy analysis to OTIS results.

5.2 Sensitivity Analysis

The energy analysis was used to perform a first order sensitivity analysis of various vehicle design parameters and flight constraints in order to illustrate the relation of these parameters to suborbital trajectory performance. This sensitivity analysis was performed by perturbing the various vehicle and trajectory parameters one at a time, recalculating the baseline and suborbital performance based on the perturbed value, and then comparing the results to the original performance shown in Figure 14. Table 3 lists the key design parameter and flightpath assumptions used to calculate performance results shown in Figure 14, giving the original values for each design parameter along with two perturbed values. The energy analysis technique was used with each perturbed value to recalculate the baseline and suborbital trajectory performance. For these energy analysis calculations, the iterative method was used resulting in the calculation of the perturbed baseline payload capacity for each case analyzed. The resulting baseline payload capacity based on each of the perturbed values is shown in Table 4.

The energy analysis results for each perturbed value in Table 3 is shown as a plot of payload ratio versus initial pullup velocity in Figures 16 through 33. For each of these figures, only the perturbed value was changed so that all other parameters were maintained at the baseline values. Each of these figures includes the original performance curve, based on the initial design parameters, shown as a dotted line, and the perturbed performance shown as a solid line. Each plot of the various perturbed values includes only suborbital trajectory performance for pullup maneuvers initiated during the airbreathing portion of the baseline ascent. As was previously mentioned, the energy analysis for suborbital trajectories initiated after the baseline transition point, is not expected to be representative of actual vehicle performance.

Table 3. Sensitivity Analysis for Design and Trajectory Parameter Assumptions (20% variations).

Design Parameter	Original Value	Decreased Value	Increased Value
Launch Vehicle Structural Mass (Structure and propellant reserve)	119,000 lbm	95,200 lbm	142,800 lbm
Launch Vehicle Average Airbreathing Specific Impulse	1,130 sec	904 sec	1,356 sec
Launch Vehicle Rocket Specific Impulse	400 sec	320 sec	480 sec
Booster Engine Specific Impulse	400 sec	320 sec	480 sec
Booster Engine Structural Mass Ratio	.10	.08	.12
Baseline Transition Velocity	22,403 ft/sec	17,923 ft/sec	25,568 ft/sec
Target Orbit Altitude	100 nm	80 nm	120 nm
Average Scramjet Dynamic Pressure	1,000 psf	800 psf	1,200 psf
Deployment Dynamic Pressure	.5 psf	.4 psf	.6 psf

Table 4. Baseline Payload Capacity Based on Perturbed Performance Parameters.

Design Parameter	Perturbed Baseline Payload Capacity	
	Parameter Decreased	Parameter Increased
Launch Vehicle Structural Mass (Structure and propellant reserve)	65,551 lbm	18,057 lbm
Launch Vehicle Average Airbreathing Specific Impulse	18,698 lbm	59,341 lbm
Launch Vehicle Rocket Specific Impulse	30,624 lbm	49,722 lbm
Booster Engine Specific Impulse	41,898 lbm	41,898 lbm
Booster Engine Structural Mass Ratio	41,898 lbm	41,898 lbm
Baseline Transition Velocity	9,244 lbm	69,630 lbm
Target Orbit Altitude	42,693 lbm	40,933 lbm
Average Scramjet Dynamic Pressure	41,943 lbm	41,860 lbm
Deployment Dynamic Pressure	41,897 lbm	41,898 lbm
Original Baseline Payload Capacity 41,898lbm		

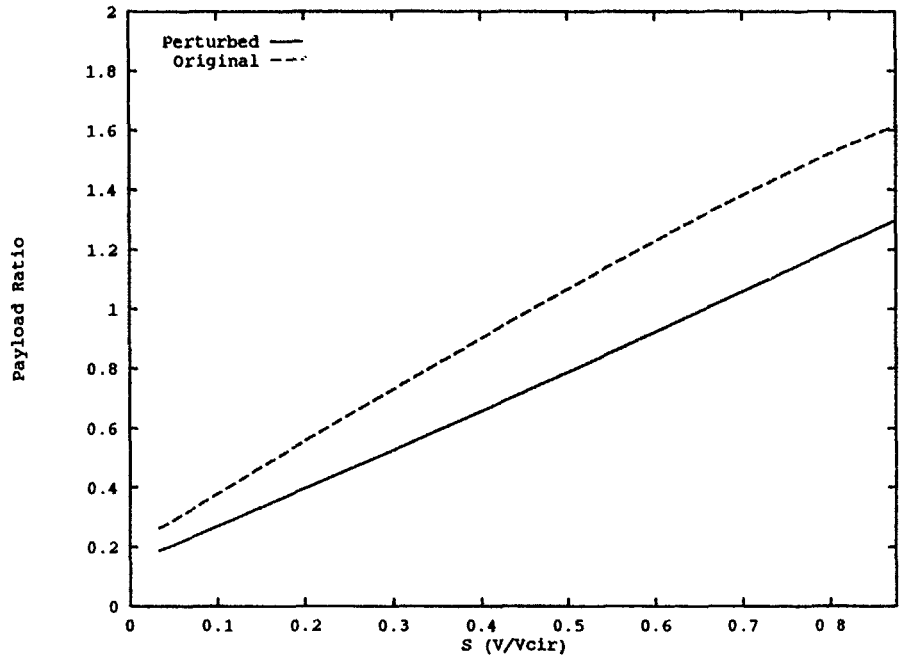

Figure 16. Sensitivity Analysis Launch Vehicle Structural Mass 95,200lbm.

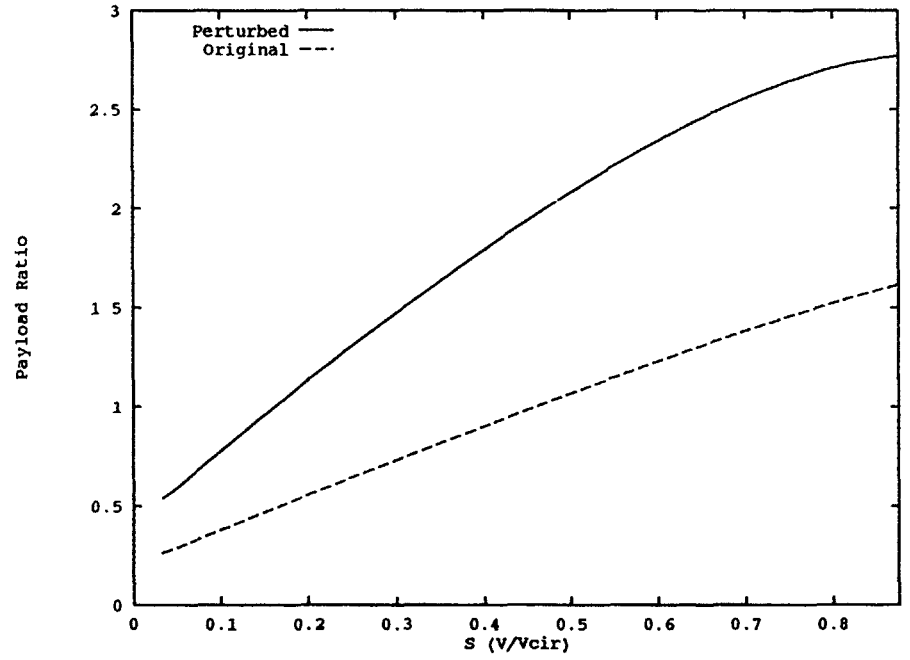

Figure 17. Sensitivity Analysis with Launch Vehicle Structural Mass 142,800lbm.

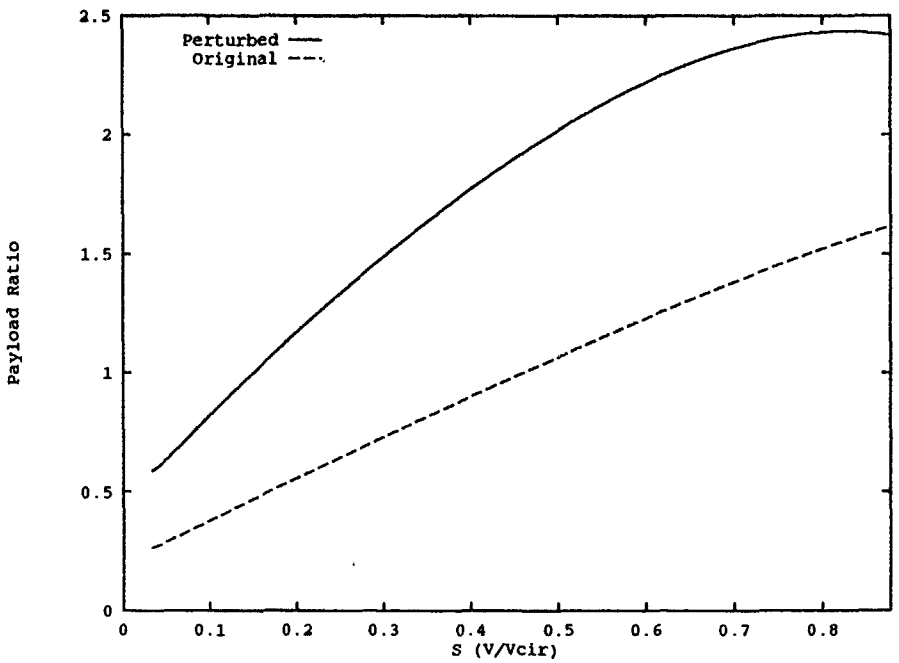

Figure 18. Sensitivity Analysis with Launch Vehicle Average Airbreathing Specific Impulse 904sec.

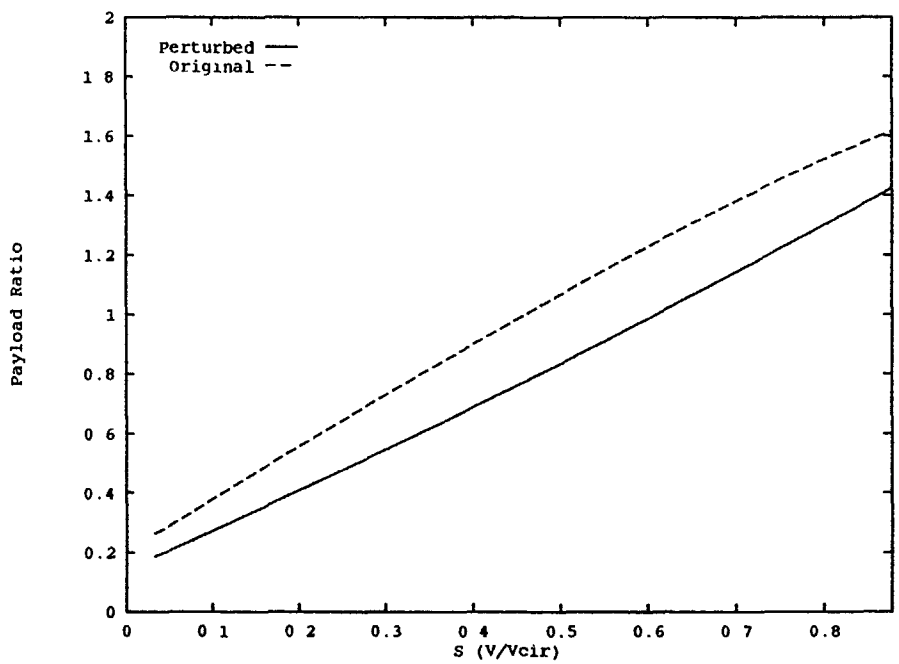

Figure 19. Sensitivity Analysis with Launch Vehicle Average Airbreathing Specific Impulse 1356sec.

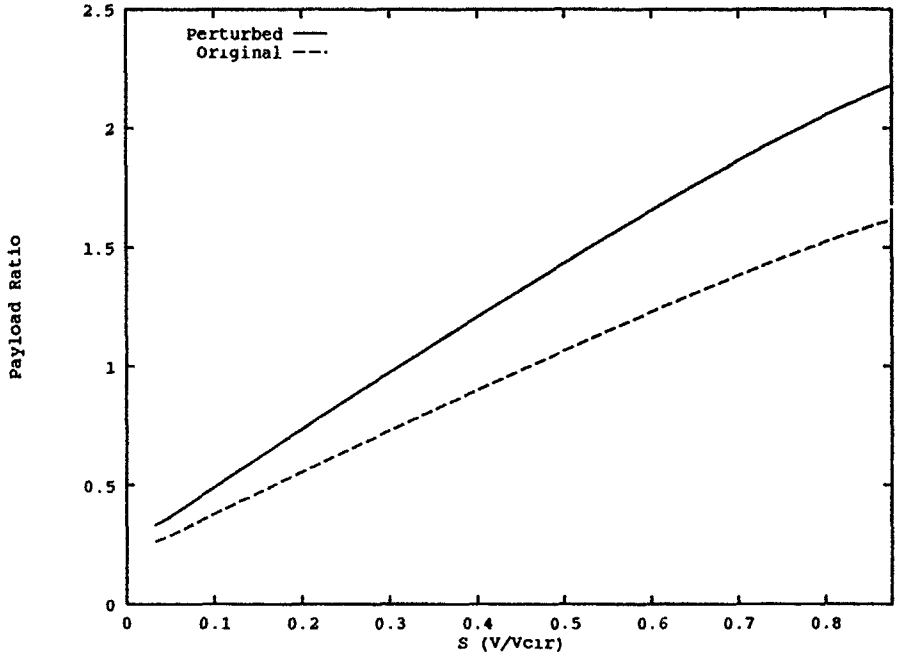

Figure 20. Sensitivity Analysis with Launch Vehicle Rocket Specific Impulse 320sec.

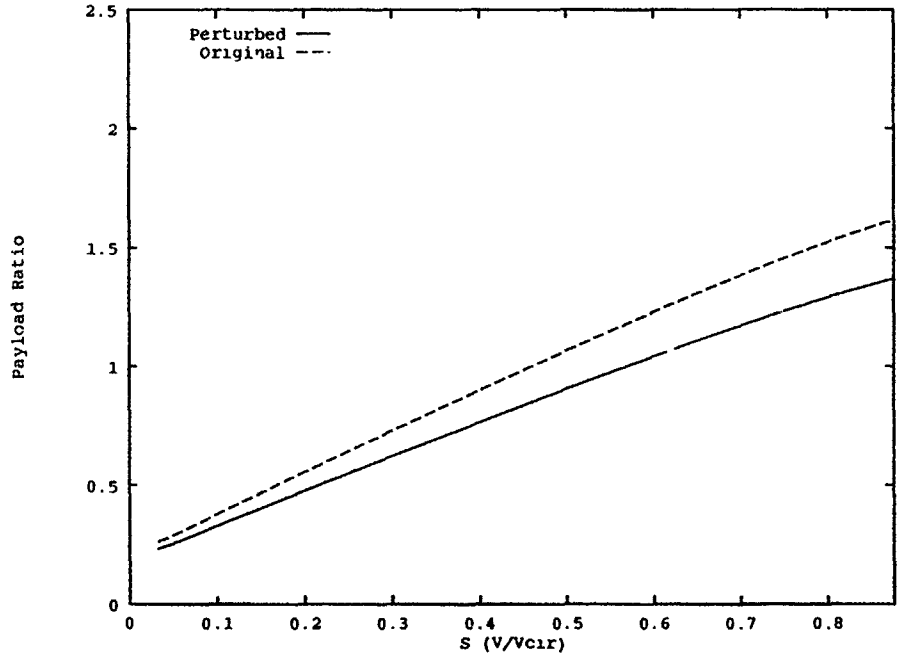

Figure 21. Sensitivity Analysis with Launch Vehicle Rocket Specific Impulse 480sec.

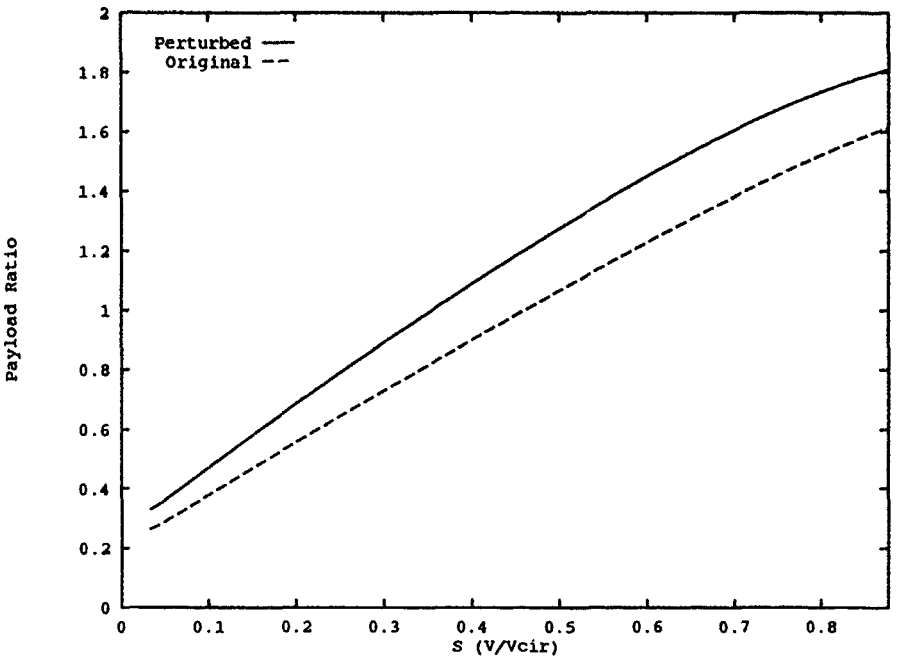

Figure 22. Sensitivity Analysis with Booster Engine Specific Impulse 320sec.

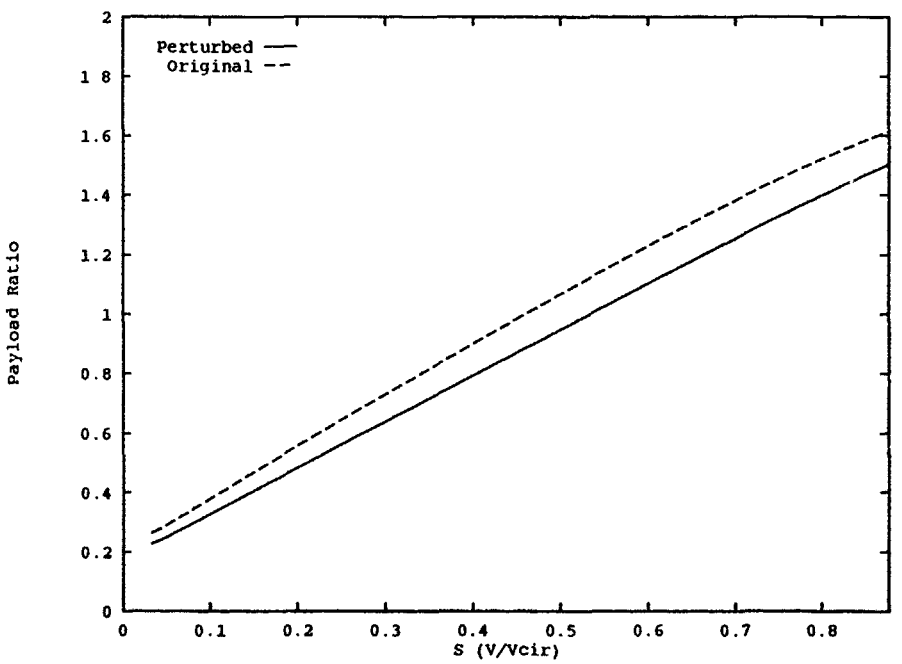

Figure 23. Sensitivity Analysis with Booster Engine Specific Impulse of 480 seconds.

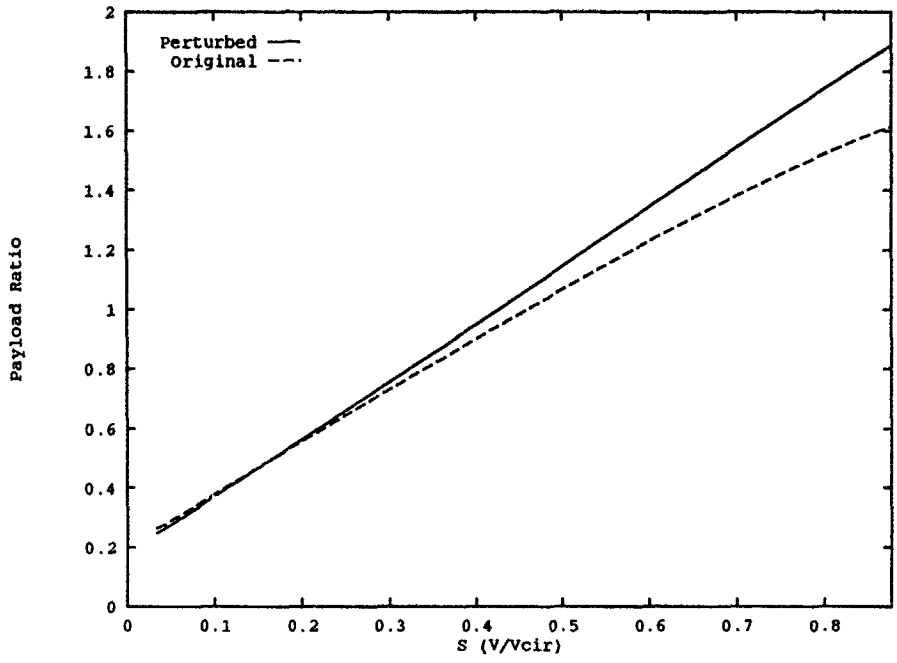

Figure 24. Sensitivity Analysis with Booster Engine Structural Mass Ratio .08.

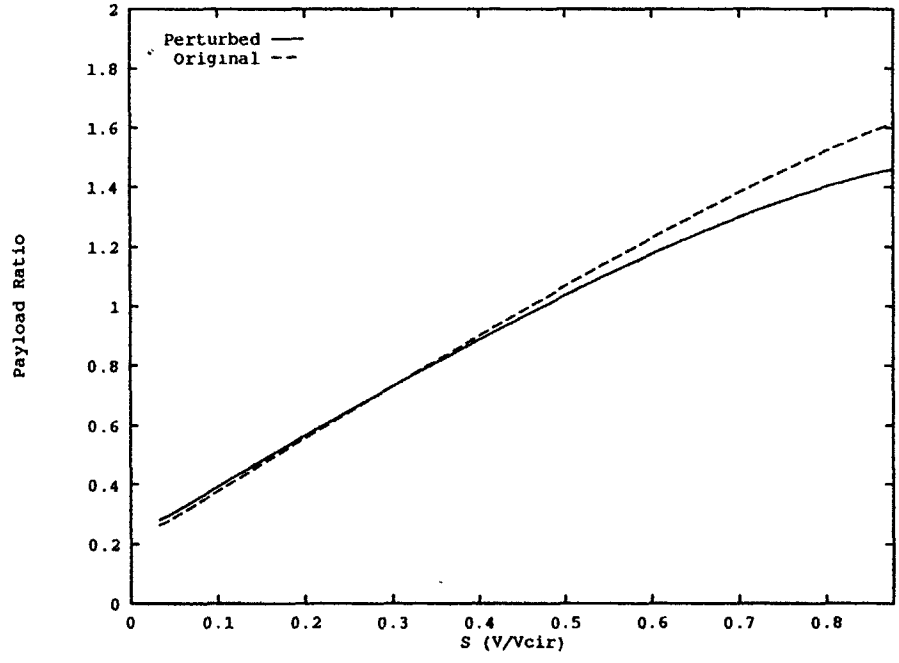

Figure 25. Sensitivity Analysis with Booster Engine Structural Mass Ratio .12.

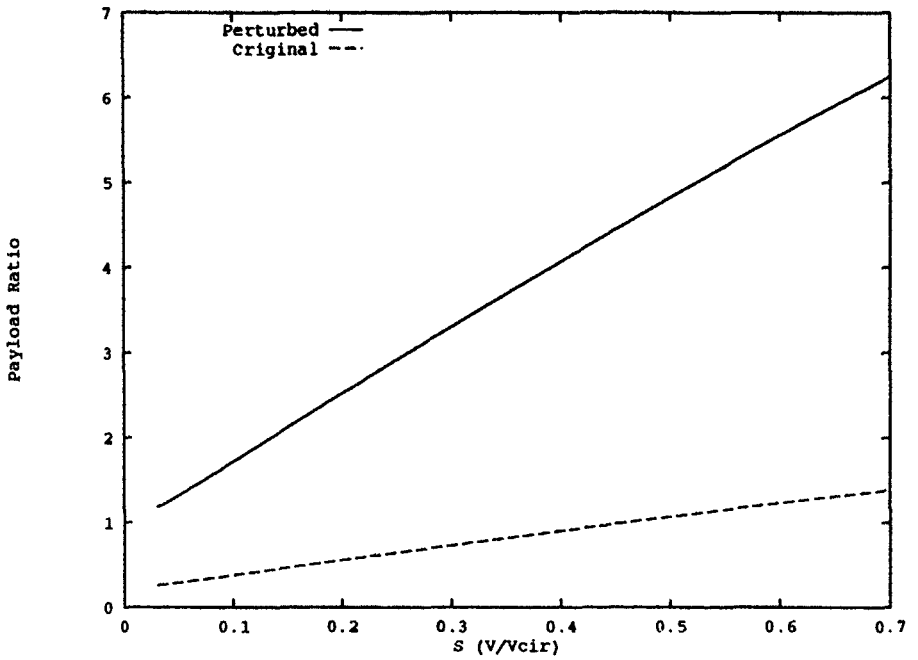

Figure 26. Sensitivity Analysis with Baseline Transition Velocity of 17,923ft/sec.

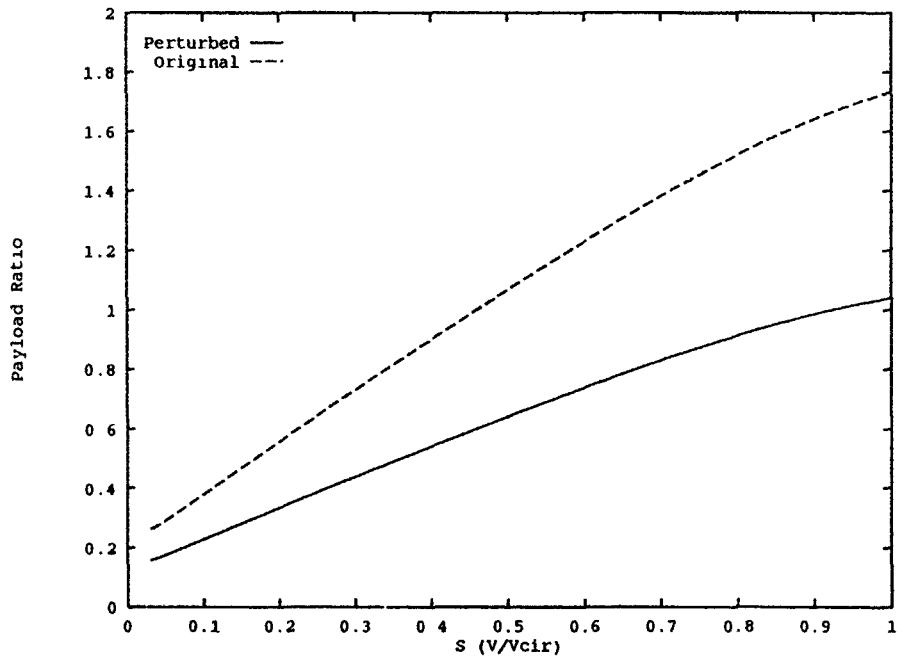

Figure 27. Sensitivity Analysis with Baseline Transition Velocity of 25,568ft/sec.

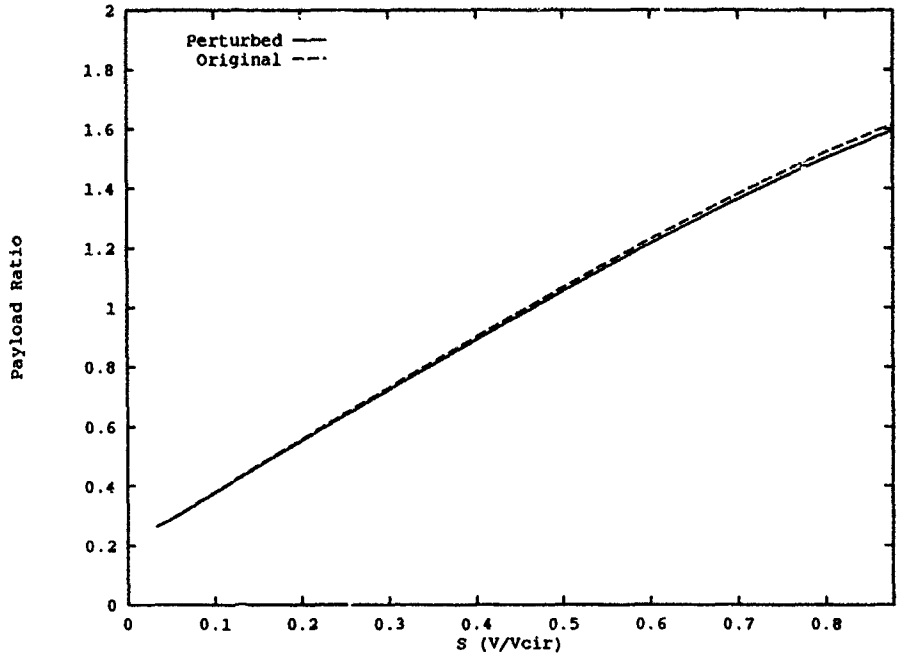

Figure 28. Sensitivity Analysis with Target Orbit Altitude of 80nm.

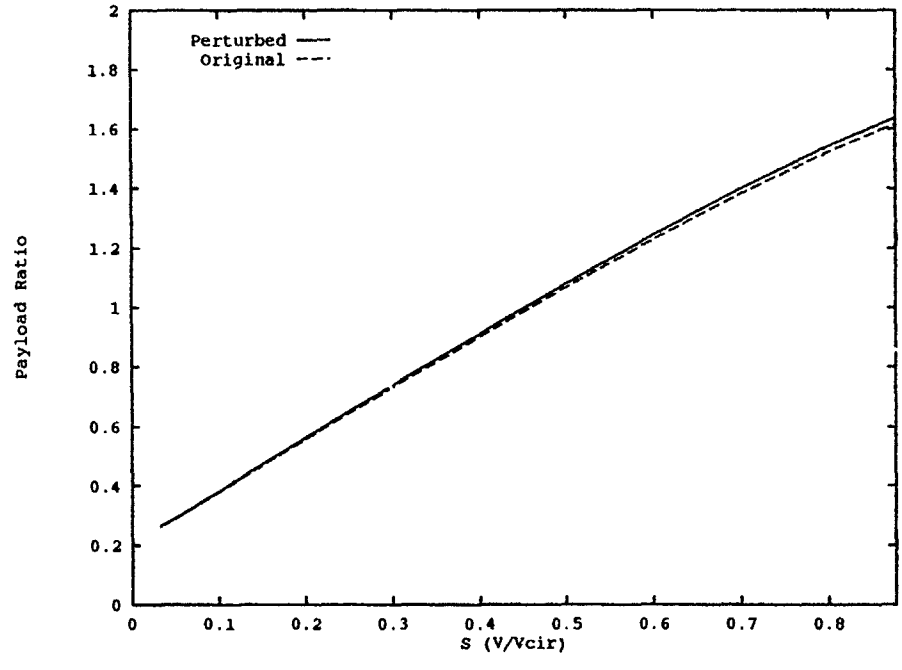

Figure 29. Sensitivity Analysis with Target Orbit Altitude of 120nm.

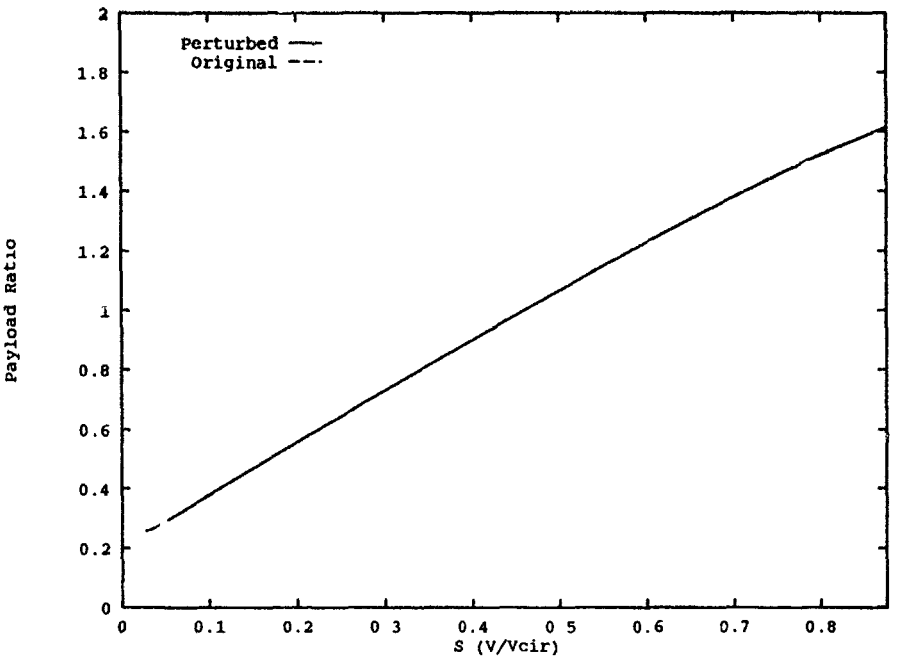

Figure 30. Sensitivity Analysis with Average Scramjet Dynamic Pressure of 800psf.

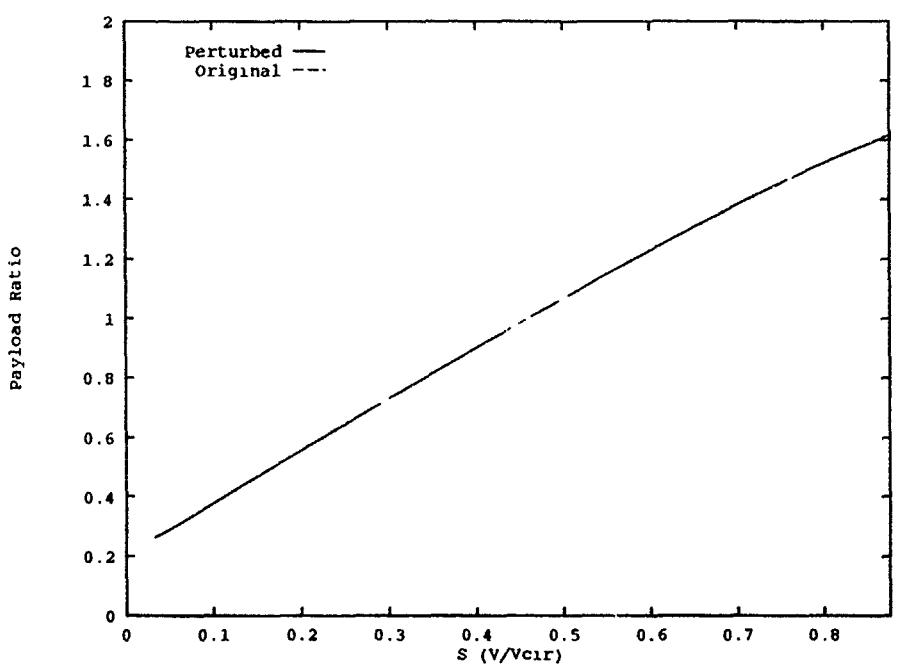

Figure 31. Sensitivity Analysis with Average Scramjet Dynamic Pressure of 1200psf.

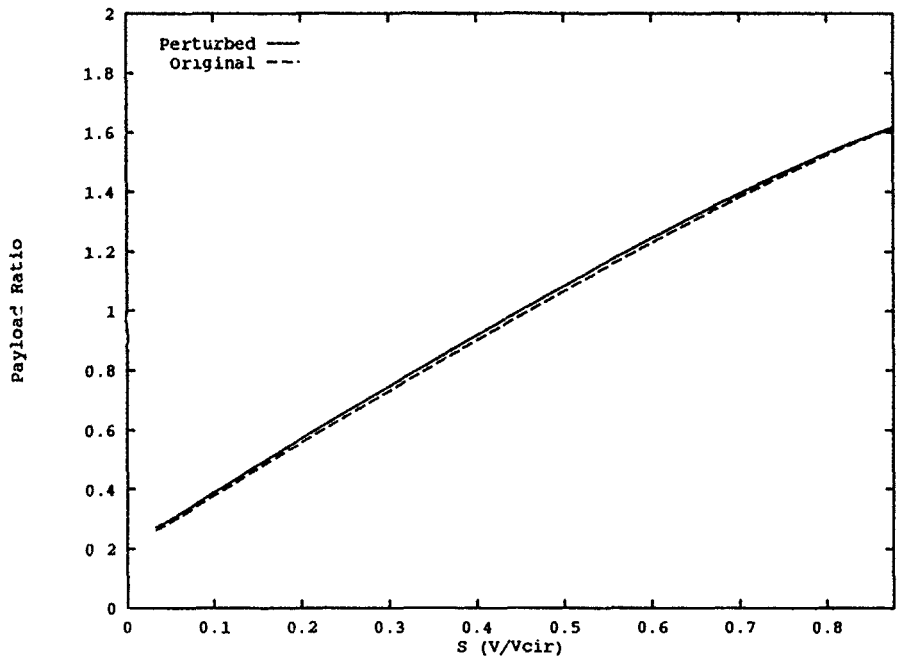

Figure 32. Sensitivity Analysis with Deployment Dynamic Pressure of .4psf.

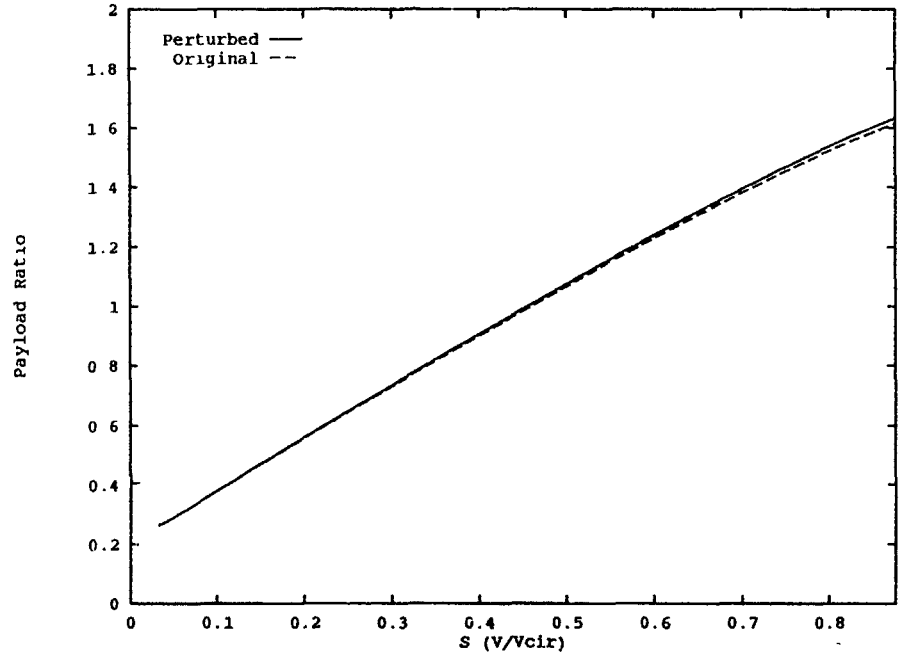

Figure 33. Sensitivity Analysis with Deployment Dynamic Pressure of .6psf.

Based on the information presented in Figures 16 - 33, the various design assumptions were listed in order of importance as shown in Table 5. Table 5 also includes the absolute percentage change between the perturbed and original performance for each design parameter. The absolute percentage change for each design parameter was determined by dividing the difference between the perturbed and original payload ratios by the original payload ratio evaluated at the baseline transition point. As shown in Table 5, the four design parameters having the most significant influence on suborbital trajectory performance were the baseline transition velocity, launch vehicle structural mass ratio, launch vehicle average airbreathing specific impulse, and the launch vehicle rocket specific impulse.

Table 5. Design Parameters Listed In Order of Importance with Percent Change in Payload Ratio Resulting from Perturbed Performance Values.

Design Parameter	Percent Change in Payload Ratio	
	Decreased Value	Increased Value
Baseline Transition Velocity	352.1%	-40.0%
Launch Vehicle Structural Mass	-19.7%	71.5%
Launch Vehicle Average Airbreathing Specific Impulse	49.7%	-11.9%
Launch Vehicle Rocket Specific Impulse	35.0%	-15.3%
Booster Engine Specific Impulse	-7.5%	5.3%
Target Orbit Altitude	-1.3%	1.3%
Booster Engine Structural Mass Ratio	0.65%	-0.65%
Average Scramjet Dynamic Pressure	-0.03%	0.03%
Deployment Dynamic Pressure	0.0%	0.0%

The information presented in Figures 16 - 33 was found to contain details that were not readily apparent from a casual review of the various plots. For this reason,

a brief discussion is presented here concerning the results shown in a few of these figures.

Figure 26 shows the sensitivity analysis results with a baseline transition velocity of 17,923 ft/sec. As shown in Table 5, it was found that the baseline transition velocity has greater impact on suborbital performance than any of the other design assumptions analyzed in this thesis. In order to fully understand the energy analysis results, it is important to remember that this analysis results in a recalculation of both the baseline and suborbital performance. For example, the original values for the various design parameters resulted in a baseline trajectory with a payload capacity of 41,898 lbm. When the original baseline transition point was changed to 17,923 ft/sec, the energy analysis calculations showed that the resulting baseline trajectory payload capacity was reduced to 9,244 lbm. The reduced baseline trajectory performance in this case was a result of the launch vehicle relying on the less efficient rocket engines for a greater portion of the ascent trajectory. The suborbital trajectory analysis based on a baseline transition at 17,923 ft/sec showed the use of suborbital flight paths could deliver payload of up to 6.2 times heavier than would be possible using the baseline trajectory (57,313 lbm payload with a suborbital trajectory initiated at the baseline transition point as compared to 9,244 lbm payload with the baseline trajectory). The significant performance increase realized by the suborbital trajectories in this case is explained by the ability of the suborbital flightpath to use the less efficient rocket engines for the acceleration of only the payload into the final orbit and not the entire structure of the launch vehicle.

The sensitivity analysis results shown in Figure 27 indicate how suborbital trajectory performance changes based on the baseline transition velocity being increased to 25,568 ft/sec. This case represents a launch vehicle that is capable of using airbreathing engines to accelerate all the way to orbital velocities. Since the launch vehicle avoids extended use of the more inefficient rocket engines in this case, the baseline trajectory performance is increased resulting in a heavier payload delivered into orbit (69,630 lbm for the perturbed baseline trajectory as compared to 41,898 lbm for the original baseline trajectory). The use of the higher efficiency airbreathing engines to a larger extent in this case results in a baseline performance greater than that of the suborbital trajectories as is indicated by the large region with a payload ratio less than 1.0.

One of the primary observations drawn from Figures 26 and 27 is that as the launch vehicle transition velocity decreases, the use of suborbital trajectories shows more and more potential. These figures also show that the best overall performance (both suborbital and baseline) can be obtained by designing a launch vehicle so as to maximize the baseline transition point. This point is indicated by the comparison of the heaviest suborbital trajectory payload capacity with a baseline transition point of 17,923 ft/sec against the baseline payload capacity with a transition point of 25,568 ft/sec (57,443 lbm as compared to 69,630 lbm).

Observations similar to those presented for Figures 26 and 27 can also be made with the other figures generated from the sensitivity analysis. In each case, if the perturbed performance parameter resulted in decreased launch vehicle performance, then the baseline payload capacity was also decreased (as shown in Table 4). In the cases where the launch vehicle performance was decreased, then the relative suborbital trajectory performance improved. The reverse of this pattern was also true, if the launch vehicle performance increased, then the suborbital trajectory performance decreased. In the cases where the payload booster motor was either increased or decreased, then the relative suborbital performance was also either increased or decreased respectively.

Another observation that can be made from the sensitivity analysis results involves the optimum initial conditions for initiation of a suborbital pullup maneuver. In nearly every sensitivity analysis result shown in Figures 16 - 33, the best suborbital trajectory performance was indicated when the initial pullup velocity coincided with the velocity of the baseline transition point. The only exception to this was shown in Figure 18 where the launch vehicle average airbreathing specific impulse was reduced from the original value. With a reduced airbreathing specific impulse, the best suborbital performance was indicated at pullup velocities slightly less than that of the baseline transition point.

VI. Conclusions and Recommendations

Based on the objectives of this project, the results presented in the previous chapters led to the following conclusions:

- The results of the two analytical methods used in this research indicated that NDV suborbital launch trajectories could be used to increase the payload weight to orbit capacity as compared to that of a standard launch profile. Based on the OTIS simulation program and the energy analysis results, suborbital trajectory performance showed a 61% increase over baseline trajectory performance.
- The results of this study indicated that in most cases, the optimum point for the initiation of a pullup maneuver coincides with the baseline transition point. By initiating a suborbital trajectory in this manner, the launch vehicle takes full advantage of improved efficiency of airbreathing engines prior to the transition to rocket propulsion for the suborbital pullup. However, the results also indicated that there were certain launch vehicle design configurations that would allow for the best suborbital performance to be obtained by initiating the suborbital pullup at speeds lower than that of the baseline transition point. Since the starting conditions for optimal suborbital pullup can be affected by various design considerations, it would be necessary to perform a separate analysis to determine the best suborbital starting conditions based on a launch vehicle design different from that used for this research.
- The amount of time available for payload deployment from a launch vehicle following a suborbital trajectory is limited. The payload weight that can be delivered to orbit from a suborbital trajectory decreases as the amount of time used for deployment increases. Results from this analysis showed deployment time periods of up to 700 seconds could be expected without degrading suborbital performance below that of the baseline ascent.
- The use of a simplified energy analysis technique was useful in estimating the relationship between various launch vehicle design parameters and suborbital launch trajectory performance. This analysis method showed that the baseline transition velocity, launch vehicle structural mass, launch vehicle airbreathing

engine efficiency, and the launch vehicle rocket engine efficiency have the largest impact on overall suborbital trajectory performance.

Since this thesis provided only a limited first look at suborbital launch trajectory performance, several areas could benefit from additional research. Topics for additional research include:

- Analysis of the reentry portion of suborbital trajectories to include propellant requirements for a return to a landing location.
- Additional research using the OTIS simulation program with improved engine and aerodynamic models based on experimental data from an actual lifting body design.
- Investigation of the operational procedures required to satisfy the short deployment times that would be encountered with suborbital launch trajectories.
- Additional research into the utility of the energy analysis technique. This research should evaluate if a correlation between the energy analysis technique and the OTIS simulation technique exists based on vehicle designs other than the one used for this analysis.
- Additional investigation into the sensitivity analysis of various launch vehicle design parameters could help in determining an ideal launch vehicle configuration.

Appendix A. *Representative Vehicle Design*

In order to produce meaningful results using the analytical methods explained in this thesis, it was necessary to perform calculations based on a specific vehicle design. The design parameters used in the different analysis methods are presented below.

For the simplified energy analysis, only a few basic physical design parameters were required along with some information on engine performance and flightpath constraints. The design parameters used for the energy analysis presented in this thesis are included in Table 6. Launch vehicle weights were based on a study presented by Kasten (7:5), and the dynamic pressure constraints were based on a study presented by Lepsch et all (10:5). Other values were selected as reasonable representations for specific impulse and transition Mach number for the baseline ascent.

Table 6. Design and Performance Parameters used for Energy Analysis.

	Design Parameter	Parameter Value
Vehicle Parameters	Gross Weight	400,000 lbm
	Empty Weight	90,000 lbm
	Total Propellant Weight	290,000 lbm
	Propellant Reserve	29,000 lbm
	Payload Weight	20,000 lbm
	Rocket *Isp*	400 sec
Booster Parameters	Booster *Isp*	400 sec
	Booster Structural Mass Fraction	0.1
Trajectory Constraints	Target orbit Altitude	100 nm
	Deployment Dynamic Pressure	0.5 psf
	Max Structural Dynamic Pressure	1200 psf
	Min Scramjet Dynamic Pressure	400 psf
	Baseline Transition Mach Number	20.75

For the trajectory analysis, using the OTIS computer program, additional information was required along with the parameters listed in Table 6. The additional

input data involved the launch vehicle aerodynamic performance, additional flight constraints and more detailed engine performance data. Efforts were taken to make all OTIS data representative of the type of performance expected from a hypersonic lifting body launch vehicle. Two different aerodynamic models were incorporated with OTIS for the vehicle lift coefficient. The first lift coefficient model was for speeds between Mach 0 to Mach 4 and was a function of speed and vehicle angle of attack as shown in Figure 34. The information used to develop this particular model was based on a study by Kauffman et all (8:21) and by Vinh (16:67-73).

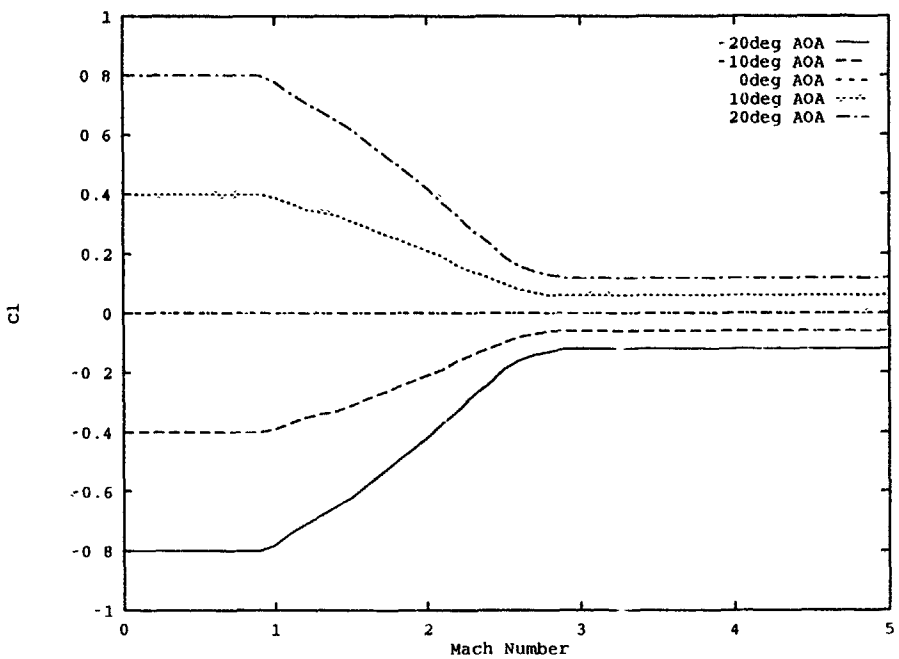

Figure 34. Low Speed Coefficient of Lift (8:21).

A high speed model for the launch vehicle coefficient of lift was developed based on *Simple Newtonian Impact Theory* resulting in the relationship shown in equation 20 as presented by Anderson (1:46-53). Equation 20 is plotted for various angles of attack in Figure 35.

$$C_l = 2\sin^2\alpha\cos\alpha \tag{20}$$

The model for aerodynamic drag was also based on the Simple Newtonian Impact Theory as presented by Anderson (1:46-53). A small change was made to this theory to allow for non-zero drag at a zero angle of attack resulting in a more

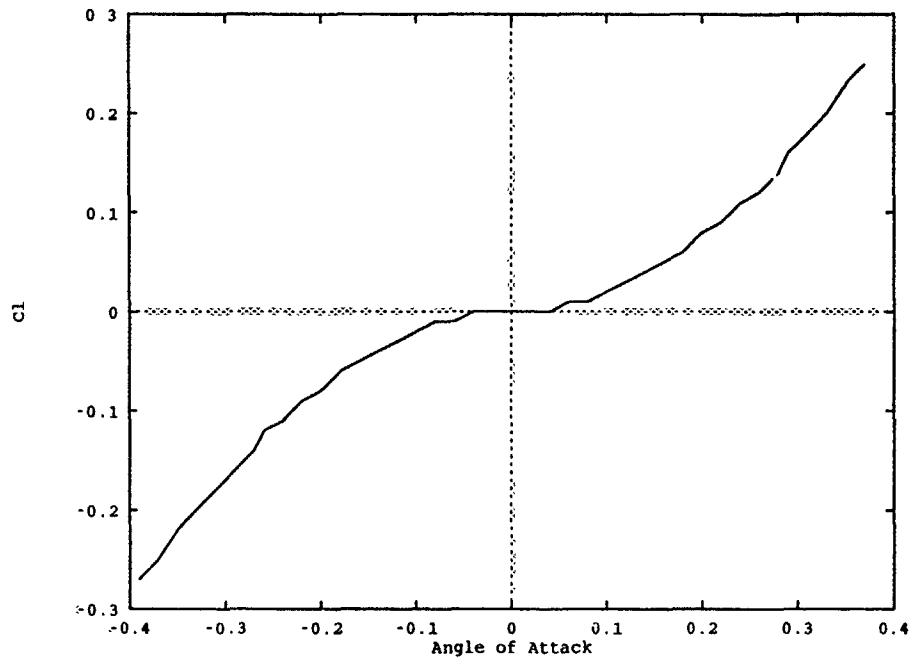

Figure 35. High Speed Coefficient of Lift.

realistic simulation. The relationship used to calculate values for the coefficient of drag is shown in equation 21 with values for the drag coefficient at zero angle of attack (Cd_o) plotted in Figure 36. Values for Cd_o are based on information presented by Kauffman (8:21).

$$C_d = Cd_o + 2\sin^3\alpha \tag{21}$$

The OTIS simulation program allowed for the use of an improved engine performance model compared to the assumption of a constant specific impulse used with the energy analysis technique. For the OTIS simulation, different specific impulse values were used to represent transitions from turbojets to ramjets, scramjets and finally to rocket propulsion. The values used to represent the various phases of engine performance are based on studies presented by Kors (9:1) and Kauffman et all (8:23-24) as shown in Figures 37 and 38.

Additional flight constraints were also incorporated in the OTIS model as indicated in Table 7. These constraints are based on studies by Lepsch et all (10:5) Berarducci (2:8) and interviews with Kasten (6).

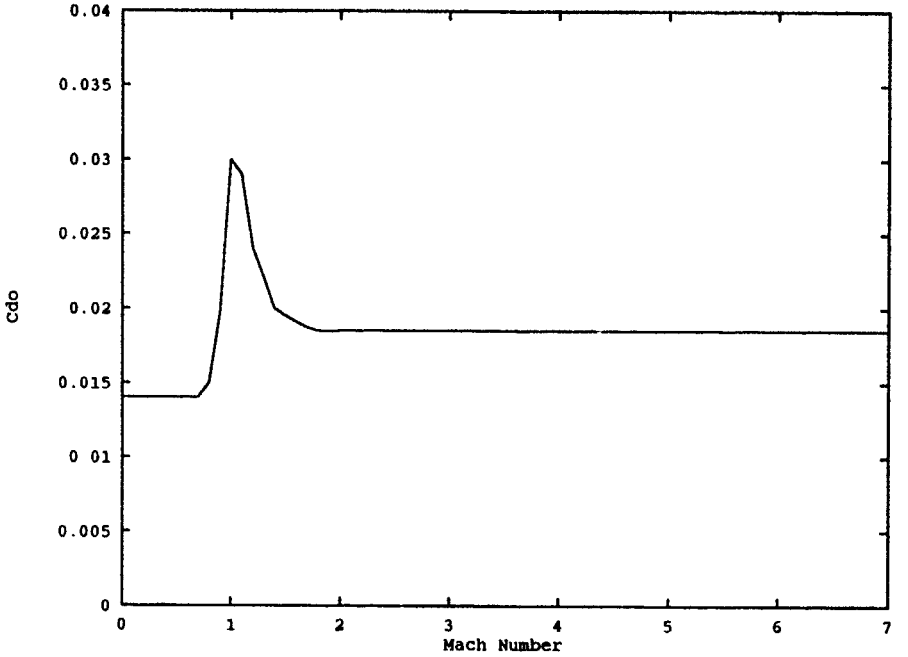

Figure 36. Zero AOA Coefficient of Drag (8:21).

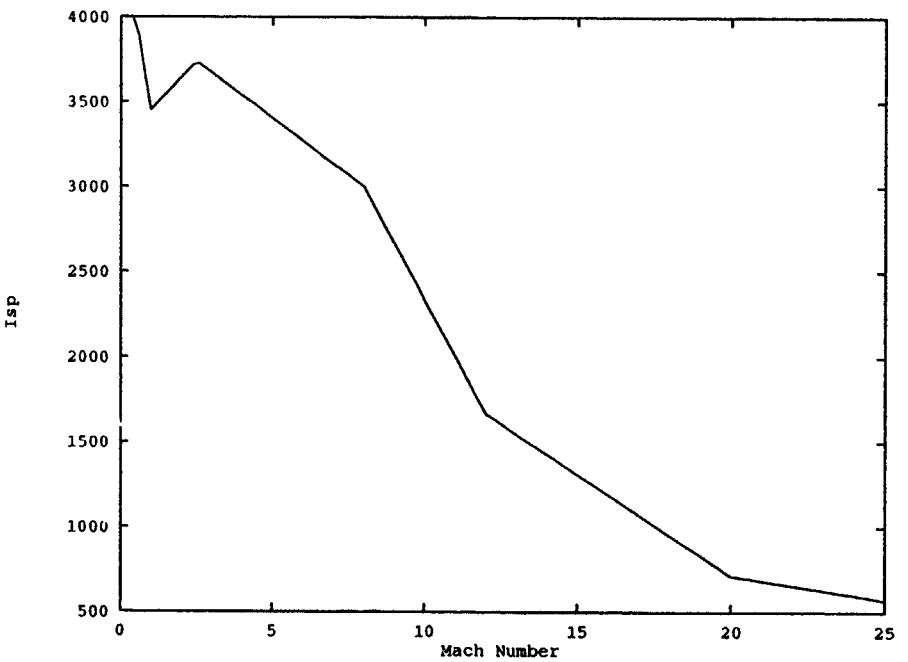

Figure 37. Airbreathing Fuel Specific Impulse (9:1).

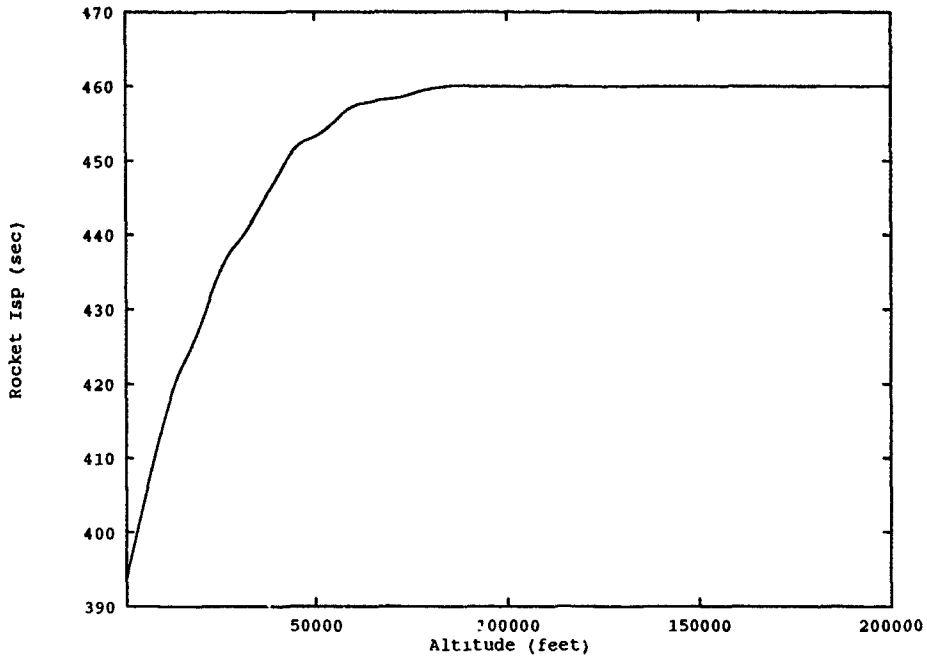

Figure 38. Rocket Fuel Specific Impulse (8:23-24).

Table 7. Vehicle Flight Constraints used with OTIS Simulation

Constraint	Value
Maximum Stagnation Temperature	4500 F
Maximum Acceleration Force	3g
Maximum Engine Thrust	250000 lbf

Appendix B. *Baseline Trajectory Data*

This appendix presents baseline performance information generated by the OTIS simulation program. This data was generated based on the representative vehicle mass parameters and flight constraints as presented in Appendix A with the exception for the baseline propellant consumption and payload weight delivered to orbit. The trajectory propellant and payload weights were determined by the OTIS program based on the aerodynamic and propulsion models used for this simulation.

The data presented in this appendix is divided into three sections: 1) Table 8 presents a summary of various performance values. 2) A tabular listing of several flight parameters with respect to time provide detailed information of the final optimized baseline trajectory developed by OTIS. A key to the flight parameter labels along with the units used is included at the end of the tabular listing. 3) Figures 39 to 43 include plots of a few flight parameters as they vary with respect to time.

Table 8. Summary of Baseline Trajectory Performance.

Performance Parameter	Value
Total Time of Flight	1932 sec
Airbreathing Time of Flight	1477 sec
Rocket Powered Time of Flight	455 sec
Total Propellant Consumption	239,102 lbm
Propellant Consumption during Air Breathing phase	186,271 lbm
Propellant Consumption during Rocket Powered phase	52,831 lbm
Transition Velocity	22403 ft/sec (Mach 20.75)
Transition Altitude	169,476 ft
Payload Weight Delivered to Orbit	41,898 lbm

TIME	ALT	VEL	WEIGHT
THRUST	GAMMA	ALPHA	LIFT
DRAG	Q	TEMP	ACCEL
0.00000000E+00	0.00000000E+00	150.00000	400000.00
260000.00	0.00000000E+00	31.785611	188688.22
44944.924	26.739991	30.275424	0.92547249
15.000000	31.291922	399.50587	399024.94
260000.00	5.2232315	9.8463818	415005.32
25315.583	189.85586	59.973669	1.2886468
30.000000	407.88037	645.90270	398044.51
260000.00	1.3513409	2.5903525	281719.36
38592.663	489.89708	83.697703	0.92316797
45.000000	1643.5090	847.03984	397018.83
260000.00	17.999256	5.0533587	911266.14
71126.079	812.29193	105.37758	2.4000637
60.000000	8616.0517	822.92052	395965.80
260000.00	42.780584	1.9135208	263430.46
49745.692	620.12583	77.539286	0.86822924
75.000000	15906.573	798.34007	394918.21
260000.00	29.530456	1.4127532	144913.44
36898.517	462.05046	48.634019	0.68245555
90.000000	21211.869	862.61319	393857.89
260000.00	24.700835	4.4223487	443107.09
42709.181	451.33888	39.047928	1.2980958
105.00000	27834.718	885.76796	392774.80
260000.00	35.292419	4.6957714	392794.91
41045.658	376.79569	19.216579	1.1915162
120.00000	35549.050	880.42404	391682.00
260000.00	33.154348	2.6598320	164655.10
31874.680	278.83721	-8.6179356	0.73617475

TIME	ALT	VEL	WEIGHT
THRUST	GAMMA	ALPHA	LIFT
DRAG	Q	TEMP	ACCEL
150.00000	43646.314	1146.2893	389429.04
260000.00	3.7984290	4.6056355	292184.62
45742.054	321.76725	33.100583	0.97292868
165.00000	44821.330	1376.8483	388303.89
260000.00	4.2598700	5.3600942	421624.72
52119.671	438.75343	80.205238	1.2657838
180.00000	46897.818	1586.3012	387206.90
260000.00	5.9523651	4.1448735	343374.77
57438.782	527.13418	129.75093	1.0708324
195.00000	49028.910	1794.4373	386121.77
260000.00	3.3664654	3.4988833	283054.93
63929.328	608.94540	185.24642	0.92515735
210.00000	50140.741	2011.4213	385049.25
260000.00	1.7608702	4.7782571	370596.73
78966.809	725.35815	249.83326	1.1209913
225.00000	51546.527	2203.7835	383990.39
260000.00	3.7022037	6.6750697	437660.73
97818.360	813.92643	312.12702	1.2881042
240.00000	54560.429	2356.5454	382942.94
260000.00	6.1896427	7.8840693	389607.91
106094.95	805.37304	363.68002	1.1788540
255.00000	58691.010	2492.9754	381899.49
260000.00	6.4455561	8.7859345	301447.44
105327.21	739.33361	410.42143	0.97757676
270.00000	62467.130	2638.9169	380853.86
260000.00	4.5871693	9.3113419	236927.70
103527.02	691.23897	462.30565	0.83553977

TIME	ALT	VEL	WEIGHT
THRUST	GAMMA	ALPHA	LIFT
DRAG	Q	TEMP	ACCEL
300.00000	65567.103	2956.6163	378738.87
260000.00	0.30915735	11.592028	284687.32
144480.90	747.89273	583.63622	0.93600323
315.00000	65633.107	3080.9410	377671.49
260000.00	1.43509992E-03	11.962023	317061.02
163517.42	809.51388	634.65789	1.0112213
330.00000	65632.160	3201.2616	376509.24
260000.00	-5.26311129E-05	11.025667	316636.08
157980.19	874.01752	685.12154	1.0064836
345.00000	65705.818	3316.7161	375522.08
260000.00	0.28389841	11.231129	346004.91
173052.93	934.79571	734.30772	1.0785660
360.00000	66329.773	3409.5396	374440.68
260000.00	1.1681837	11.356383	358635.49
179960.92	957.93007	773.38716	1.1126707
375.00000	67751.177	3501.7852	373355.61
260000.00	1.8920333	10.734346	333421.18
164694.01	942.18926	810.82637	1.0512359
390.00000	69575.381	3615.2472	372266.45
260000.00	1.9079368	9.9351915	300740.55
146771.64	918.19795	856.41349	0.97371155
405.00000	71147.005	3753.1327	371172.15
260000.00	1.2635271	9.0531857	273464.43
133821.25	916.26267	912.86150	0.90944150
417.97646	71853.230	3889.2349	370220.53
260000.00	0.32621732	8.2446525	258354.74
129098.31	950.52742	970.66778	0.87041148

TIME	ALT	VEL	WEIGHT
THRUST	GAMMA	ALPHA	LIFT
DRAG	Q	TEMP	ACCEL
420.00000	71939.525	3892.2474	370071.73
259994.14	0.99818353	13.481412	556085.13
231187.22	947.99465	971.73478	1.6674529
435.00000	74781.143	3935.6563	368968.14
259998.72	4.4949058	12.618805	436221.84
184855.00	843.85389	981.90011	1.3491901
450.00000	80226.133	4018.2039	367862.28
260000.19	5.7797443	11.954312	314874.95
136349.24	675.64829	998.99206	1.0524425
465.00000	86479.997	4143.0880	366752.58
260000.12	5.4204109	11.662496	236336.55
103614.49	531.85295	1027.3791	0.88884305
480.00000	91798.343	4310.6101	365637.38
260000.00	4.0482480	11.911796	206832.95
89715.180	446.86756	1072.3534	0.84288367
495.00000	95530.289	4499.2537	364514.90
260000.09	2.6397969	12.658768	212194.21
89824.717	408.00785	1128.6742	0.86449745
510.00000	98003.064	4694.2851	363384.58
260000.16	1.5272952	13.598991	235756.14
97817.816	395.29619	1190.7184	0.92151781
525.00000	99568.797	4884.6723	362246.07
260000.38	0.90074022	14.411968	264858.49
108936.78	397.65408	1253.9061	0.99161867
540.00000	100698.70	5062.8459	361099.21
259999.82	0.81799994	14.807225	283977.28
116710.79	405.14679	1313.6822	1.0396193

TIME	ALT	VEL	WEIGHT
THRUST	GAMMA	ALPHA	LIFT
DRAG	Q	TEMP	ACCEL
570.00000	103293.19	5408.0085	358781.58
259999.79	1.0783279	14.575064	278574.37
114511.46	409.44818	1423.1425	1.0321724
585.00000	104829.54	5585.6355	357610.65
260000.00	1.1145833	14.329975	267900.08
110236.51	406.58832	1475.9071	1.0100262
600.00000	106398.61	5770.2094	356431.60
260000.33	1.0158289	14.213732	260951.35
107463.24	402.20534	1529.1804	0.99743410
615.00000	107846.81	5958.8838	355244.28
260000.60	0.88678719	14.206591	259141.75
106723.98	399.79725	1583.1959	0.99689729
630.00000	109176.93	6149.8321	354048.44
260000.49	0.77180206	14.245015	260161.09
107112.56	399.31840	1637.4517	1.0028281
645.00000	110396.21	6341.2912	352843.86
259999.70	0.71288786	14.265761	261577.91
107679.94	400.38656	1691.4258	1.0094745
660.00000	111589.46	6533.2924	351630.39
259998.34	0.69526855	14.233461	261113.90
107514.02	401.39816	1744.4618	1.0116134
675.00000	112793.47	6726.7754	350407.87
259997.09	0.69175229	14.163121	258922.97
106671.91	401.79030	1796.5530	1.0097012
690.00000	114015.15	6922.4669	349176.11
259996.65	0.68575480	14.075042	255712.84
105434.67	401.54023	1847.8653	1.0054701

TIME	ALT	VEL	WEIGHT
THRUST	GAMMA	ALPHA	LIFT
DRAG	Q	TEMP	ACCEL
720.00000	116473.33	7322.4463	346683.93
259999.49	0.63015402	13.912632	249247.36
102952.98	400.12839	1949.1489	0.99721697
735.00000	117663.52	7526.4695	345423.07
260000.84	0.59331033	13.844527	246739.01
102004.80	399.82298	1999.5556	0.99482617
750.00000	118817.69	7732.8417	344152.17
260000.33	0.55921135	13.782410	244703.32
101248.39	399.93890	2049.8575	0.99352664
765.00000	119939.08	7941.2520	342873.15
259998.84	0.53411756	13.723752	242992.68
100625.27	400.38783	2099.9640	0.99297448
780.00000	121048.04	8151.6004	341584.37
259999.11	0.51845902	13.663496	241202.25
99974.880	400.78974	2149.6351	0.99227973
795.00000	122155.59	8364.0798	340276.90
259999.95	0.50849470	13.595601	239025.96
99179.988	400.96964	2198.8110	0.99076210
810.00000	123272.40	8578.8919	338941.73
259999.91	0.50037111	13.514026	236170.85
98129.856	400.76121	2247.4231	0.98777482
825.00000	124394.00	8796.5394	337574.31
259999.72	0.48643946	13.416856	232669.67
96842.919	400.30268	2295.6740	0.98339378
840.00000	125504.19	9017.2233	336173.88
259999.99	0.46562160	13.313320	229026.33
95513.651	399.91299	2343.8378	0.97878233

TIME	ALT	VEL	WEIGHT
THRUST	GAMMA	ALPHA	LIFT
DRAG	Q	TEMP	ACCEL
870.00000	127640.17	9467.4322	333267.64
259999.67	0.41652221	13.131206	223247.85
93450.658	400.22478	2440.5751	0.97333023
885.00000	128667.16	9696.2747	331758.08
259998.47	0.40210560	13.062349	221357.83
92797.844	400.84545	2488.9932	0.97308787
900.00000	129691.29	9927.4950	330207.43
259997.35	0.39672891	12.992284	219358.43
92103.754	401.33016	2537.0919	0.97275548
915.00000	130731.28	10161.320	328612.92
259997.01	0.39702645	12.904436	216551.80
91110.259	401.36699	2584.6608	0.97075030
930.00000	131798.70	10398.245	326971.76
259997.97	0.39596428	12.784514	212419.29
89631.322	400.79660	2631.6477	0.96590557
945.00000	132871.03	10639.128	325280.41
259999.74	0.38318260	12.641526	207536.18
87892.969	400.09237	2678.6016	0.95953698
960.00000	133923.61	10883.951	323534.59
260000.96	0.36184077	12.498110	202852.19
86249.330	399.68702	2725.8921	0.95381372
975.00000	134932.47	11132.644	321729.9
260000.03	0.33585894	12.377076	199261.52
85026.840	399.99084	2773.8904	0.95071148
990.00000	135895.04	11334.463	319862.16
259996.37	0.31783202	12.292386	197149.37
84349.727	400.98873	2822.4755	0.95110307

TIME	ALT	VEL	WEIGHT
THRUST	GAMMA	ALPHA	LIFT
DRAG	Q	TEMP	ACCEL
1020.0000	137823.96	11896.429	315912.81
259994.56	0.32252181	12.131860	192962.98
83007.343	402.49122	2918.9083	0.95284480
1035.0000	138855.84	12157.418	313817.28
260002.45	0.33464213	11.991978	188441.94
81481.382	401.91415	2965.8576	0.94885267
1050.0000	139927.22	12423.513	311620.34
260003.91	0.33187992	11.795146	181972.13
79313.647	400.67616	3012.4394	0.94094570
1065.0000	140989.68	12695.105	309328.23
259995.42	0.31269239	11.580854	175194.00
77101.525	399.64149	3059.5436	0.93275181
1080.0000	141998.74	12972.007	306955.70
259979.68	0.28312796	11.393472	169716.04
75390.108	399.55063	3107.8966	0.92765413
1095.0000	142920.18	13253.656	304522.97
259964.62	0.25393766	11.274270	166873.43
74599.395	400.94028	3157.9979	0.92832990
1110.0000	143801.49	13538.361	302060.91
259969.90	0.24810521	11.209621	165827.48
74397.495	402.89115	3208.6499	0.93306384
1125.0000	144707.06	13826.431	299563.61
259985.86	0.26143218	11.138877	164384.92
74047.599	404.31750	3258.7744	0.93727402
1140.0000	145698.36	14118.436	297020.94
259999.08	0.28635823	10.999867	160382.25
72841.752	404.19770	3307.3420	0.93641631

TIME	ALT	VEL	WEIGHT
THRUST	GAMMA	ALPHA	LIFT
DRAG	Q	TEMP	ACCEL
1170.0000	147923.96	14721.298	291777.52
259994.71	0.28749746	10.424580	143012.29
67510.496	400.02364	3401.3988	0.91667616
1185.0000	148987.30	15033.722	289071.38
259988.95	0.25188683	10.124424	134768.84
65111.330	398.95650	3450.3676	0.90860346
1200.0000	149906.84	15352.855	286303.26
259988.36	0.20550594	9.9320346	130296.81
63974.098	400.35720	3502.6386	0.90801466
1215.0000	150698.82	15675.923	283468.12
259994.43	0.18473226	9.8841684	130191.37
64190.610	403.80590	3557.3763	0.91588829
1230.0000	151490.81	16002.081	280561.50
260001.77	0.19993452	9.8805143	131168.79
64693.409	407.12996	3611.9495	0.92639564
1245.0000	152400.70	16332.275	277579.51
260003.91	0.23958902	9.7976452	129433.24
64314.512	408.37593	3664.1814	0.93242268
1260.0000	153532.99	16667.916	274518.53
259994.49	0.28665158	9.5156910	121519.81
62051.137	405.85535	3712.1518	0.92756855
1275.0000	154801.91	17013.348	271373.78
259977.51	0.29121495	9.0413107	108700.30
58543.288	401.29336	3758.3811	0.91496397
1290.0000	156048.22	17368.694	268133.12
259963.38	0.25670376	8.5390446	96533.263
55574.693	398.83800	3807.8763	0.90486177

TIME	ALT	VEL	WEIGHT
THRUST	GAMMA	ALPHA	LIFT
DRAG	Q	TEMP	ACCEL
1320.0000	157946.94	18104.123	261312.43
259973.07	0.15203531	8.1229368	88421.773
54187.625	403.14406	3920.4622	0.91320243
1335.0000	158714.90	18478.424	257709.86
259996.51	0.16400188	8.2410118	92046.310
55382.632	407.90035	3980.3059	0.93044971
1350.0000	159611.27	18857.725	253961.50
260012.49	0.21485266	8.2644871	93173.095
55859.589	410.58445	4037.6664	0.94523819
1365.0000	160812.32	19244.097	250052.96
260000.47	0.28063823	7.9182589	85204.761
53967.154	408.49816	4089.1761	0.94705497
1380.0000	162252.61	19643.371	245970.25
259954.20	0.29051591	7.0464504	66828.342
49682.518	402.95010	4137.0798	0.93716967
1395.0000	163553.86	20058.451	241687.34
259917.89	0.21404323	5.9904983	48158.155
46137.647	399.88606	4189.7280	0.93223975
1410.0000	164437.26	20486.629	237171.47
259935.40	9.27691162E-02	5.2214840	37039.004
44768.729	403.36954	4252.6495	0.93824667
1425.0000	164615.84	20924.983	232384.79
260030.40	2.83125218E-02	5.2079323	38183.380
46359.997	417.97023	4331.9277	0.95270172
1440.0000	164163.74	21365.565	227240.21
260063.65	-3.10842699E-02	6.1656928	56512.851
51648.861	443.30727	4425.1975	0.98344815

TIME	ALT	VEL	WEIGHT
THRUST	GAMMA	ALPHA	LIFT
DRAG	Q	TEMP	ACCEL
1470.0000	167123.06	22222.256	216224.30
259497.78	0.71829762	9.9577384	140180.27
68674.232	428.56859	4518.0708	1.2164405
1476.6486	169475.85	22403.414	213729.36
259224.52	1.0730066	10.952584	157395.75
71692.821	400.00004	4500.0001	1.2909004
1476.6486	169475.85	22403.414	213729.36
280000.00	1.0730066	14.746424	278207.59
114337.23	400.00004	4500.0001	1.7914986
1485.0000	174412.82	22616.811	208643.39
280122.98	1.9050320	13.547079	202774.81
84206.055	342.48887	4434.2931	1.5708955
1500.0000	188993.89	23098.133	199526.47
278638.65	2.8602952	11.639647	93047.947
40836.890	210.18968	4208.7137	1.3829240
1515.0000	208132.48	23671.853	190559.02
263283.17	3.3432104	10.343415	37262.641
17696.993	105.82145	3894.8555	1.3417693
1530.0000	229915.42	24192.401	183132.39
181474.83	3.5751632	9.6060347	13727.001
6946.0310	45.008369	3511.4097	0.96938604
1545.0000	252942.15	24460.606	179296.11
55852.884	3.6259453	8.7350336	4096.0002
2294.7753	16.182629	3065.1625	0.30332395
1560.0000	275965.55	24487.004	178570.18
434.16673	3.5528544	6.7179413	797.33709
636.50577	5.2813182	2613.6822	4.88673667E-03

TIME	ALT	VEL	WEIGHT
THRUST	GAMMA	ALPHA	LIFT
DRAG	Q	TEMP	ACCEL
1590.0000	320073.50	24426.094	178610.82
691.12847	3.3392477	8.6384037	118.10379
67.048812	0.47695330	1822.2478	3.66706319E-03
1605.0000	341057.68	24399.884	178602.48
-78.791570	3.2305077	10.750830	57.561881
26.560057	0.15166020	1519.9968	6.29655873E-04
1620.0000	361321.09	24374.308	178598.80
390.35189	3.1202363	8.0762002	11.089030
6.8461919	5.11366012E-02	1270.3592	2.15744209E-03
1635.0000	380858.22	24350.336	178587.57
220.40760	3.0088347	-1.3271779	-0.16735706
2.0597918	2.00549472E-02	1081.0553	1.22266262E-03
1650.0000	399663.62	24326.604	178585.04
-36.252915	2.8962917	-10.252272	-3.4257439
1.6384002	9.89738619E-03	951.97158	2.09620249E-04
1665.0000	417732.31	24303.658	178584.56
95.377261	2.7827734	-11.323804	-2.3907951
1.0659441	5.69579235E-03	858.46325	5.31041947E-04
1680.0000	435060.14	24281.945	178580.77
111.37353	2.6682929	-2.1250178	-5.60444325E-02
0.37456860	3.63125392E-03	786.80204	6.21574876E-04
1695.0000	451643.70	24261.064	178578.56
18.765082	2.5530423	5.4235556	0.24630994
0.27889051	2.48875895E-03	729.60245	1.03667049E-04
1710.0000	467479.62	24240.975	178578.43
-1.3667090	2.4369488	2.0200979	2.53614257E-02
0.18544880	1.79958967E-03	682.54893	8.68792595E-06

TIME	ALT	VEL	WEIGHT
THRUST	GAMMA	ALPHA	LIFT
DRAG	Q	TEMP	ACCEL
1740.0000	496894.54	24203.676	178578.42
-1.19795495E-02	2.2023722	-1.5278900	-1.01464200E-02
0.10878632	1.05867957E-03	609.40779	6.78473874E-07
1755.0000	510467.15	24186.487	178578.34
4.7997505	2.0839721	-5.1571307	-7.60993898E-02
9.39765401E-02	8.49256790E-04	580.36420	2.63959650E-05
1770.0000	523279.22	24170.276	178578.19
3.2143167	1.9648820	-10.069609	-0.23323116
0.11318886	6.97751959E-04	555.11090	1.76591015E-05
1785.0000	535328.01	24155.027	178578.19
-1.4867107	1.8451479	-13.522663	-0.34546889
0.14352221	5.85515234E-04	533.06784	8.89817027E-06
1800.0000	546610.92	24140.771	178577.97
12.294432	1.7247967	-14.356373	-0.33066488
0.13604234	5.00099495E-04	513.63914	6.85960588E-05
1815.0000	557125.53	24127.482	178577.90
-11.382437	1.6038849	-12.949654	-0.23583655
9.91192860E-02	4.34197283E-04	496.53604	6.39998899E-05
1830.0000	566869.73	24115.179	178577.73
119.20850	1.4824437	-10.759004	-0.14540245
6.70565667E-02	3.82541224E-04	481.44896	6.67327700E-04
1845.0000	575839.78	24105.456	178558.01
994.89518	1.3599006	-10.039412	-0.11352846
5.52344213E-02	3.41625685E-04	468.19890	5.57163796E-03
1860.0000	584031.43	24097.164	178532.85
-36.452463	1.2369028	-10.883370	-0.12008154
5.49351307E-02	3.08955270E-04	456.58600	2.04354344E-04

TIME	ALT	VEL	WEIGHT
THRUST	GAMMA	ALPHA	LIFT
DRAG	Q	TEMP	ACCEL
1890.0000	598037.70	24145.468	177718.24
58504.051	0.95873951	-12.383058	-0.13110042
5.59315950E-02	2.62923274E-04	439.47036	0.32919539
1905.0000	603363.84	24429.766	174177.23
161328.02	0.69963261	-12.554944	-0.12960527
5.50178170E-02	2.53159961E-04	440.88614	0.92622897
1920.0000	606739.88	24985.757	167547.86
239822.61	0.33310077	-13.065625	-0.14079249
5.90189132E-02	2.54831657E-04	452.51487	1.4313676
1931.7010	607611.55	25567.709	160898.44
280000.00	6.75453901E-10	-13.686308	-0.15952036
6.60957468E-02	2.64221640E-04	467.94751	1.7402281

Key to Parameters

Parameter	Units	Description
TIME	seconds	Simulation Time
ALT	feet	Altitude
VEL	ft/sec	Flight Velocity
WEIGHT	lb mass	Vehicle Weight
THRUST	lb force	Vehicle Thrust
GAMMA	degrees	Flightpath Angle
ALPHA	degrees	Vehicle Angle of Attack
LIFT	lb force	Aerodynamic Lift Force
DRAG	lb force	Aerodynamic Drag Force
Q	lb force	Dynamic Pressure
TEMP	deg F	Stagnation Temperature
ACCEL	gs	Total Vehicle Acceleration

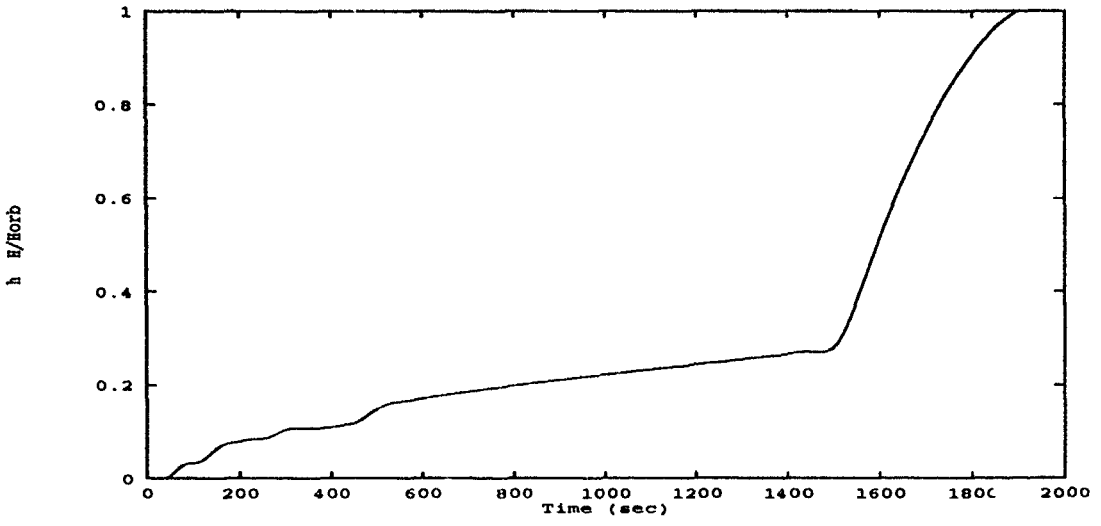

Figure 39. Baseline Trajectory Altitude versus Time.

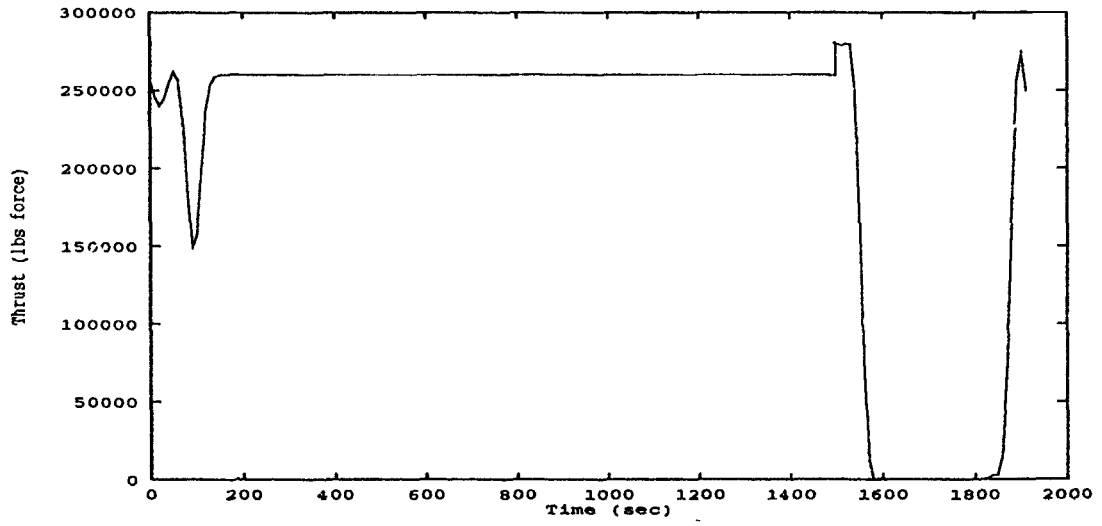

Figure 40. Baseline Trajectory Thrust versus Time.

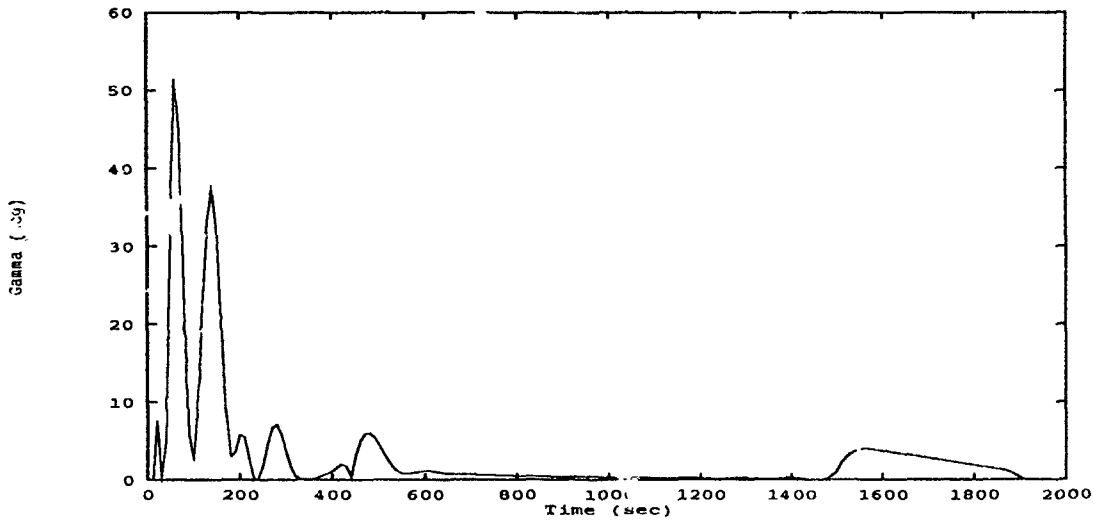

Figure 41. Baseline Trajectory Flight Path Angle versus Time.

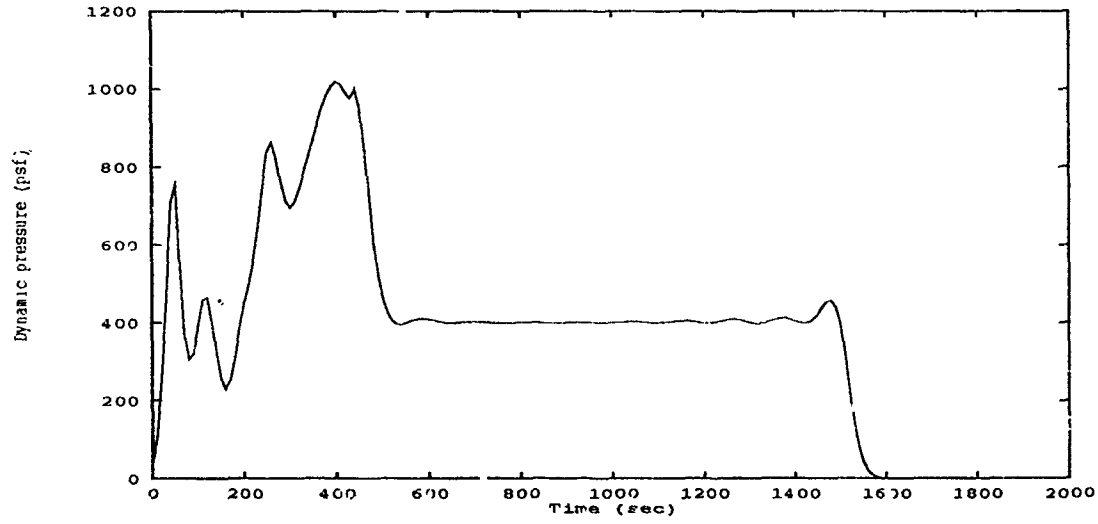

Figure 42. Baseline Trajectory Dynamic Pressure versus Time.

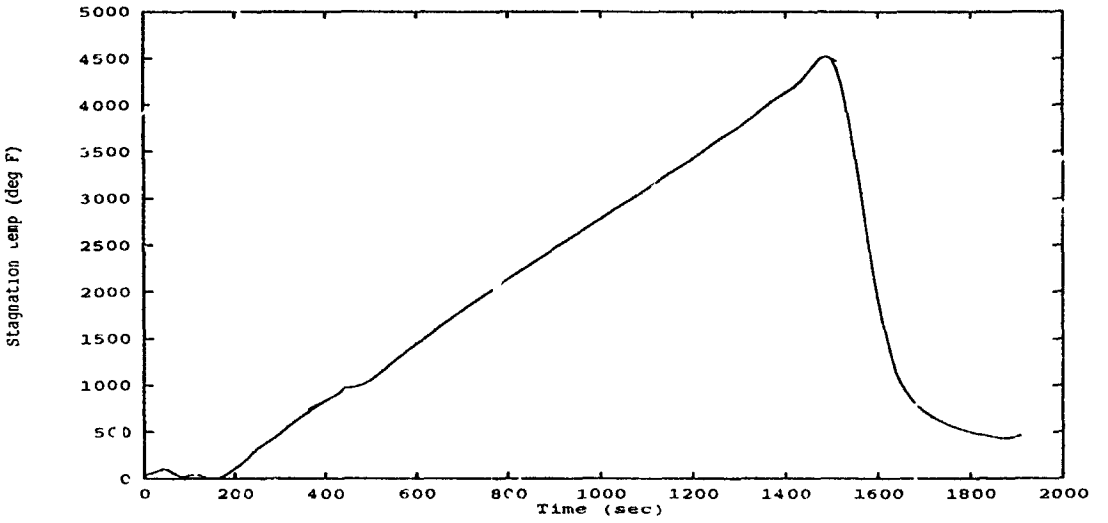

Figure 43. Baseline Trajectory Temperature versus Time.

Appendix C. *Suborbital Trajectory Data*

This appendix presents suborbital trajectory performance information generated by the OTIS simulation program. This appendix only includes information for a specific suborbital trajectory beginning at the point where the launch vehicle performs a pullup maneuver causing a deviation from the baseline trajectory. Performance information for the portion of the ascent trajectory prior to the pullup maneuver is found in Appendix B.

The data listed in this appendix does not include any portion of the reentry phase of the launch vehicle. The OTIS analysis was used to simulate launch vehicle performance only up to the point of payload separation. Performance information for portions of the trajectory after payload separation apply only to the final payload and booster motor combination.

The data presented in the appendix is divided into three sections: 1) Table 9 presents a summary of various performance values. 2) A tabular listing of several flight parameters with respect to time provide detailed information of the final optimized suborbital trajectory developed by OTIS. A key to the flight parameter labels along with the units used is included at the end of the tabular listing. 3) Figures 44 to 48 include plots of a few flight parameters as they vary with respect to time.

Table 9. Summary of Suborbital Trajectory Performance.

Performance Parameter	Value
Total Time of Flight	2443 sec
Time of Flight prior to Pullup	1478 sec
Time of Flight from Pullup to Separation	135 sec
Time for Payload Separation	30 sec
Time of Flight from Separation to Orbit Insertion	800 sec
Total Launch Vehicle Propellant Consumption	186,271 lbm
Total Booster Engine Propellant Consumption	24,631 lbm
Suborbital Trajectory Apogee Height	329,942 ft
Booster Engine Empty Weight	2,463 lbm
Payload Weight Delivered to Orbit	67,635 lbm

TIME	ALT	VEL	WEIGHT
THRUST	GAMMA	ALPHA	LIFT
DRAG	Q	TEMP	ACCEL
1476.0000	169475.85	22403.400	213729.40
0.00000000E+00	1.0730000	17.611452	387289.08
164128.63	399.99954	4499.9975	1.9680573
1486.0000	176017.09	22164.527	213729.40
8.38046078E-15	2.2494084	18.172417	318576.00
136557.53	310.64990	4320.4474	1.6217245
1496.0000	186391.10	21976.853	213729.40
-?.84826048E-14	3.0734860	18.188085	215235.80
92290.954	209.54958	4075.0142	1.0957225
1506.0000	199072.68	21850.481	213729.40
7.40974622E-14	3.5044769	17.737794	126013.44
53537.271	128.45378	3798.9348	0.64059819
1516.0000	212738.66	21770.327	213729.40
-6.64272375E-14	3.6432766	17.178008	68851.960
28942.885	74.445188	3516.8552	0.34945077
1526.0000	226525.02	21718.202	213729.40
1.49865705E-14	3.6057110	16.587956	36335.066
15134.599	41.913251	3242.6645	0.18416306
1536.0000	239935.47	21682.282	213729.40
2.64532613E-14	3.4684996	15.750149	18264.325
7540.3365	23.209095	2981.4984	9.24515353E-02
1546.0000	252695.27	21655.685	213729.40
1.52600714E-13	3.2770024	14.851817	9045.5442
3717.7564	12.832405	2738.6341	4.57576438E-02
1556.0000	264662.45	21634.243	213729.40
-7.83691598E-14	3.0588796	14.253994	4709.3725
1938.7996	7.2197309	2519.3232	2.38285010E-02

TIME	ALT	VEL	WEIGHT
THRUST	GAMMA	ALPHA	LIFT
DRAG	Q	TEMP	ACCEL
1576.0000	285978.25	21600.153	213729.40
1.61894686E-13	2.5881318	12.195595	1176.3868
504.93018	2.4292215	2144.1790	5.98968593E-03
1586.0000	295272.36	21586.124	213729.40
-1.76722406E-13	2.3451791	11.160005	597.30979
268.73344	1.4637428	1986.1600	3.06452158E-03
1596.0000	303641.97	21573.700	213729.40
9.07932114E-14	2.1000460	10.475490	334.15049
157.15412	0.92586595	1851.4502	1.72770510E-03
1606.0000	311082.47	21562.757	213729.40
6.76234088E-14	1.8536240	5.7559398	68.232467
69.856014	0.61305778	1736.4981	4.56886369E-04
1611.4489	314744.32	21557.410	213729.40
2.43805426E-22	1.7187800	-0.92535304	-3.1467009
51.340201	0.50000011	1681.7715	2.40661990E-04
1611.4489	314744.32	21557.410	213729.40
0.00000000E+00	1.7187800	-6.8084066	-77.549286
60.626753	0.50000011	1681.7715	4.60560090E-04
1616.0000	317590.27	21553.258	213729.40
0.00000000E+00	1.6060238	-2.3184905	-7.7595637
44.088686	0.42650158	1640.0282	2.09453245E-04
1626.0000	323164.61	21545.112	213729.40
0.00000000E+00	1.3583474	11.771863	141.29496
61.645892	0.31229792	1560.5278	7.21273403E-04
1636.0000	327805.33	21538.300	213729.40
0.00000000E+00	1.1107717	14.657186	165.88613
68.179449	0.24124936	1496.9460	8.39148102E-04

TIME	ALT	VEL	WEIGHT
THRUST	GAMMA	ALPHA	LIFT
DRAG	Q	TEMP	ACCEL
1641.4489	329942.05	21535.144	94729.400
82179.440	0.97585225	12.806960	0.20584767
8.68102146E-02	0.21483891	1469.0335	0.86751738
1646.0000	331587.93	21660.453	93896.018
85479.170	0.94130675	12.689513	0.18720639
7.91833679E-02	0.19885430	1456.8960	0.91035951
1656.0000	335075.95	21960.525	91938.875
92375.561	0.88934937	12.429970	0.15325941
6.52929468E-02	0.16935670	1433.7035	1.0047494
1666.0000	338469.52	22289.134	89847.400
98160.163	0.86734370	12.165775	0.12625626
5.42474660E-02	0.14537916	1413.7204	1.0925206
1676.0000	341868.90	22639.610	87669.050
102068.92	0.87166805	11.893731	0.10396396
4.51278995E-02	0.12502686	1395.1099	1.1642524
1686.0000	345374.34	23005.283	85451.282
103337.78	0.89870073	11.610641	8.50183292E-02
3.73632894E-02	0.10[illegible]315	1376.1970	1.2093178
1696.0000	349086.09	23379.482	83241.554
101202.67	0.94482006	11.313308	6.85802983E-02
3.05935019E-02	9.08400631E-02	1355.3340	1.2157709
1706.0000	353100.44	23749.636	81117.081
95031.030	1.0034806	10.999139	5.41440091E-02
2.45919914E-02	7.57419835E-02	1330.4910	1.1715291
1716.0000	357442.21	24094.219	79187.440
85370.252	1.0637448	10.670957	4.16610856E-02
1.93265261E-02	6.18082037E-02	1300.0371	1.0780781

TIME	ALT	VEL	WEIGHT
THRUST	GAMMA	ALPHA	LIFT
DRAG	Q	TEMP	ACCEL
1736.0000	366994.05	24678.005	76011.903
60268.743	1.1739740	9.9953136	2.30815773E-02
1.12714566E-02	3.88790143E-02	1224.3081	0.79288550
1746.0000	372145.67	24903.954	74809.737
47180.178	1.2169224	9.6592701	1.71221825E-02
8.61914670E-03	3.08241918E-02	1184.9968	0.63066887
1756.0000	377508.77	25077.113	73893.762
35301.181	1.2470846	9.3320247	1.27430673E-02
6.63503929E-03	2.45379521E-02	1145.4771	0.47772877
1766.0000	383016.08	25201.708	73230.639
25546.419	1.2649910	9.0215369	9.54813324E-03
5.15489665E-03	1.96476913E-02	1106.3339	0.34884873
1776.0000	388602.57	25289.886	72754.172
17864.889	1.2742094	8.7440802	7.25576084E-03
4.06006784E-03	1.58773918E-02	1068.6552	0.24555136
1786.0000	394236.82	25348.177	72430.193
11982.652	1.2762574	8.5178471	5.62533920E-03
3.24836950E-03	1.29625420E-02	1032.7981	0.16543721
1796.0000	399887.38	25383.110	72224.533
7625.7702	1.2726528	8.3610301	4.47464188E-03
2.64386452E-03	1.06958835E-02	998.95565	0.10558418
1806.0000	405522.82	25401.214	72103.024
4520.3064	1.2649131	8.2918217	3.67171765E-03
2.19215215E-03	8.92167807E-03	967.26711	6.26923045E-02
1816.0000	411112.62	25408.945	72031.989
2392.9567	1.2545310	8.3279353	3.12624231E-03
1.85633326E-03	7.53143904E-03	938.01921	3.32207302E-02

TIME	ALT	VEL	WEIGHT
THRUST	GAMMA	ALPHA	LIFT
DRAG	Q	TEMP	ACCEL
1836.0000	422123.32	25407.015	71975.596
230.65485	1.2286988	8.5971417	2.44003529E-03
1.39323834E-03	5.52079022E-03	885.48111	3.20461172E-03
1846.0000	427538.41	25400.604	71974.752
-108.89302	1.2140271	8.6828159	2.15873544E-03
1.21805114E-03	4.78976098E-03	861.95923	1.51294580E-03
1856.0000	432887.92	25392.711	71981.602
-152.58361	1.1987269	8.6341775	1.86630370E-03
1.06014316E-03	4.18703253E-03	840.01632	2.11976908E-03
1866.0000	438167.80	25384.946	71988.244
-49.325470	1.1832049	8.3749564	1.54706039E-03
9.12194711E-04	3.68587121E-03	819.54430	6.85197263E-04
1876.0000	443375.23	25378.511	71988.782
57.737780	1.1677768	7.8269595	1.20018504E-03
7.71815312E-(	3.26719897E-03	800.50332	8.02030224E-04
1886.0000	448512.74	25372.587	71987.241
112.42049	1.1522897	6.8829845	8.31111423E-04
6.39621275E-04	2.91272030E-03	782.63520	1.56166494E-03
1896.0000	453580.21	25366.924	71984.848
125.83582	1.1366885	5.4133780	4.63905521E-04
5.26958701E-04	2.61115946E-03	765.86512	1.74808098E-03
1906.0000	458577.04	25361.412	71982.147
110.84896	1.1209471	3.2879023	1.54770967E-04
4.44379865E-04	2.35196322E-03	750.03213	1.53994471E-03
1916.0000	463502.65	25355.939	71979.684
80.325064	1 1050397	0.37631965	1.15495802E-05
3.93859154E-04	2.12880342E-03	735.11875	1.11593530E-03

TIME	ALT	VEL	WEIGHT
THRUST	GAMMA	ALPHA	LIFT
DRAG	Q	TEMP	ACCEL
1936.0000	473137.64	25344.753	71977.226
22.392048	1.0726600	-8.2504343	-7.19859563E-04
4.32323151E-04	1.76575591E-03	707.61549	3.11094561E-04
1946.0000	477845.50	25339.121	71976.850
7.3801437	1.0562429	-13.644400	-1.74922277E-03
7.25244094E-04	1.61745803E-03	694.92059	1.02530908E-04
1956.0000	482479.43	25333.522	71976.753
-0.12091308	1.0396865	-19.105866	-3.00984614E-03
1.31710580E-03	1.48647375E-03	682.82452	1.68410931E-06
1966.0000	487038.82	25327.981	71976.820
-2.3295783	1.0229878	-24.107021	-4.18025857E-03
2.12071408E-03	1.37075217E-03	671.33013	3.23689117E-05
1976.0000	491523.10	25322.523	71976.933
-1.4643079	1.0061436	-28.120051	-5.03284998E-03
2.87659405E-03	1.26854673E-03	660.44452	2.03465781E-05
1986.0000	495931.68	25317.172	71976.979
0.25841995	0.98915098	-30.618021	-5.39297937E-03
3.29749158E-03	1.17704845E-03	650.02427	3.59012306E-06
1996.0000	500263.92	25311.925	71976.966
1.2648653	0.97201128	-31.358147	-5.22333093E-03
3.25461724E-03	1.09500123E-03	640.05598	1.75725548E-05
2006.0000	504519.26	25306.775	71976.941
1.5446618	0.95472954	-30.788818	-4.72565621E-03
2.90220607E-03	1.02176442E-03	630.58645	2.14596164E-05
2016.0000	508697.14	25301.721	71976.910
1.3205942	0.93731010	-29.461495	-4.10284770E-03
2.43326814E-03	9.55655248E-04	621.51111	1.83461902E-05

TIME	ALT	VEL	WEIGHT
THRUST	GAMMA	ALPHA	LIFT
DRAG	Q	TEMP	ACCEL
2036.0000	516818.33	25291.897	71976.864
0.25200470	0.90207550	-26.738727	-3.06746069E-03
1.68500816E-03	8.42276119E-04	604.57378	3.49979513E-06
2046.0000	520760.55	25287.126	71976.861
-0.15166396	0.88426853	-26.431591	-2.83210396E-03
1.54171849E-03	7.93115426E-04	596.59824	2.10926217E-06
2056.0000	524623.17	25282.451	71976.864
-0.31276611	0.86633653	-27.123828	-2.79301102E-03
1.55157614E-03	7.48472795E-04	588.96933	4.34709081E-06
2066.0000	528405.70	25277.873	71976.869
-0.30059966	0.84828123	-28.461654	-2.86754173E-03
1.65472753E-03	7.08126005E-04	581.72149	4.17781456E-06
2076.0000	532107.66	25273.394	71976.875
-0.19255618	0.83010497	-30.066204	-2.98111921E-03
1.79671546E-03	6.70936595E-04	574.71185	2.67654076E-06
2086.0000	535728.55	25269.013	71976.880
-6.60272661E-02	0.81181007	-31.558611	-3.07223362E-03
1.92392989E-03	6.37170599E-04	568.04439	9.19157875E-07
2096.0000	539267.89	25264.732	71976.883
1.59551942E-03	0.79339887	-32.560009	-3.07966718E-03
1.97653434E-03	6.05966539E-04	561.60070	5.54164223E-08
2106.0000	542725.21	25260.551	71976.884
-5.59543490E-02	0.77487431	-32.740478	-2.96215202E-03
1.90936249E-03	5.77444404E-04	555.44989	7.78988986E-07
2116.0000	546100.05	25256.470	71976.890
-0.20509312	0.75624025	-32.209396	-2.75068391E-03
1.75045822E-03	5.51194219E-04	549.54800	2.84999746E-06

TIME	ALT	VEL	WEIGHT
THRUST	GAMMA	ALPHA	LIFT
DRAG	Q	TEMP	ACCEL
2136.0000	552600.62	25248.610	71976.905
-0.43243965	0.71865281	-30.379998	-2.28241139E-03
1.38696613E-03	5.04755418E-04	538.47264	6.00873473E-06
2146.0000	555725.50	25244.833	71976.911
-0.33708402	0.69970391	-29.768536	-2.11525983E-03
1.26484880E-03	4.84135793E-04	533.26487	4.68401241E-06
2156.0000	558766.21	25241.159	71976.914
1.33320100E-02	0.68065454	-29.817133	-2.03780142E-03
1.22010825E-03	4.65123286E-04	528.28692	1.87521689E-07
2166.0000	561722.34	25237.589	71976.901
0.64131605	0.66150473	-30.724239	-2.06250306E-03
1.26456012E-03	4.47529797E-04	523.51835	8.90962639E-06
2176.0000	564593.48	25234.126	71976.872
1.3319456	0.64225674	-32.152760	-2.14544802E-03
1.36341661E-03	4.31190790E-04	518.93979	1.85050481E-05
2186.0000	567379.29	25230.768	71976.834
1.8154855	0.62291576	-33.641967	-2.23413758E-03
1.47094839E-03	4.16061608E-04	514.56196	2.52234010E-05
2196.0000	570079.41	25227.513	71976.799
1.8222004	0.60348700	-34.731130	-2.27771833E-03
1.53710875E-03	4.02040725E-04	510.37783	2.53170046E-05
2206.0000	572693.48	25224.361	71976.774
1.0823554	0.58397563	-34.959520	-2.22830606E-03
1.51137346E-03	3.89007168E-04	506.37151	1.50381409E-05
2216.0000	575221.15	25221.308	71976.777
-0.65868129	0.56438732	-33.871019	-2.04686478E-03
1.35477419E-03	3.76858738E-04	502.52944	9.15114540E-06

TIME	ALT	VEL	WEIGHT
THRUST	GAMMA	ALPHA	LIFT
DRAG	Q	TEMP	ACCEL
2236.0000	580016.26	25215.472	71977.018
-2.1810898	0.52499499	-27.745307	-1.37730434E-03
7.78910461E-04	3.55149494E-04	495.38247	3.03032639E-05
2246.0000	582282.99	25212.735	71977.021
3.2896489	0.50517305	-23.554999	-1.01209960E-03
5.04742976E-04	3.45422765E-04	492.05525	4.57033486E-05
2256.0000	584462.00	25210.158	71976.756
16.524006	0.48525298	-19.210508	-6.87943671E-04
3.01805585E-04	3.36404851E-04	488.89696	2.29573377E-04
2266.0000	586552.91	25207.770	71976.082
40.228722	0.46522406	-15.159920	-4.32977237E-04
1.78108187E-04	3.28014045E-04	485.89235	5.58917106E-04
2276.0000	588555.26	25205.633	71974.691
76.454566	0.44508114	-11.831528	-2.63583809E-04
1.14708455E-04	3.20203110E-04	483.03702	1.06224156E-03
2286.0000	590468.53	25203.852	71972.097
117.35763	0.42485496	-9.3550128	-1.63343116E-04
8.48285264E-05	3.12996210E-04	480.35262	1.63059824E-03
2296.0000	592292.64	25202.309	71968.868
147.43629	0.40457970	-7.6289563	-1.07050028E-04
7.11855864E-05	3.06293720E-04	477.80997	2.04861127E-03
2306.0000	594027.59	25200.869	71965.669
150.98956	0.38428320	-6.5459228	-7.76078432E-05
6.44456358E-05	3.00089888E-04	475.41300	2.09807685E-03
2316.0000	595673.36	25199.395	71963.167
112.31646	0.36401329	-5.9984768	-6.40595842E-05
6.12159272E-05	2.94339851E-04	473.15000	1.56074853E-03

TIME	ALT	VEL	WEIGHT
THRUST	GAMMA	ALPHA	LIFT
DRAG	Q	TEMP	ACCEL
2336.0000	598699.44	25195.113	71966.282
-131.80525	0.32380521	-6.0837422	-6.35798976E-05
5.93646532E-05	2.84098489E-04	468.99041	1.83148695E-03
2346.0000	600083.03	25191.526	71975.715
-194.13171	0.30400164	-6.5256891	-7.18505188E-05
5.99540288E-05	2.79529953E-04	467.06040	2.69718420E-03
2356.0000	601376.88	25188.940	71980.757
10.421261	0.28383137	-7.1248522	-8.41417356E-05
6.15210351E-05	2.75340977E-04	465.28113	1.44777726E-04
2366.0000	602577.18	25189.323	71971.761
663.59006	0.26274457	-7.8010673	-9.91699360E-05
6.40189058E-05	2.71584075E-04	463.71870	9.22014418E-03
2376.0000	603680.10	25194.639	71939.078
1947.1111	0.24019139	-8.4741702	-1.15292435E-04
6.69740057E-05	2.68286461E-04	462.42885	2.70661105E-02
2386.0000	604681.71	25206.914	71872.764
4042.4370	0.21559345	-9.0640828	-1.30234056E-04
6.99358220E-05	2.65483244E-04	461.47165	5.62443504E-02
2396.0000	605570.63	25230.760	71749.679
7038.8005	0.18723793	-9.5187379	-1.42151470E-04
7.25599047E-05	2.63314680E-04	461.00289	9.81021878E-02
2406.0000	606325.79	25269.902	71552.285
10801.122	0.15432188	-9.8542003	-1.51240625E-04
7.47668056E-05	2.61884879E-04	461.14557	0.15095426
2416.0000	606926.14	25326.747	71270.116
15160.870	0.11678481	-10.096696	-1.58186108E-04
7.65982832E-05	2.61283441E-04	461.98968	0.21272408

TIME	ALT	VEL	WEIGHT
THRUST	GAMMA	ALPHA	LIFT
DRAG	Q	TEMP	ACCEL
2436.0000	607578.04	25503.172	70409.580
24998.518	2.76056759E-02	-10.407688	-1.68871811E-04
7.98187757E-05	2.62989158E-04	466.15981	0.35504427
2441.4489	607611.55	25567.709	70098.101
27799.068	8.31643238E-11	-10.473689	-1.71757243E-04
8.07913292E-05	2.64221640E-04	467.94751	0.39657376

Key to Parameters

Parameter	Units	Description
TIME	seconds	Simulation Time
ALT	feet	Altitude
VEL	ft/sec	Flight Velocity
WEIGHT	lbs mass	Vehicle Weight
THRUST	lbs force	Vehicle Thrust
GAMMA	degrees	Flightpath Angle
ALPHA	degrees	Vehicle Angle of Attack
LIFT	lbs force	Aerodynamic Lift Force
DRAG	lbs force	Aerodynamic Drag Force
Q	lbs force	Dynamic Pressure
TEMP	deg F	Stagnation Temperature
ACCEL	gs	Total Vehicle Acceleration

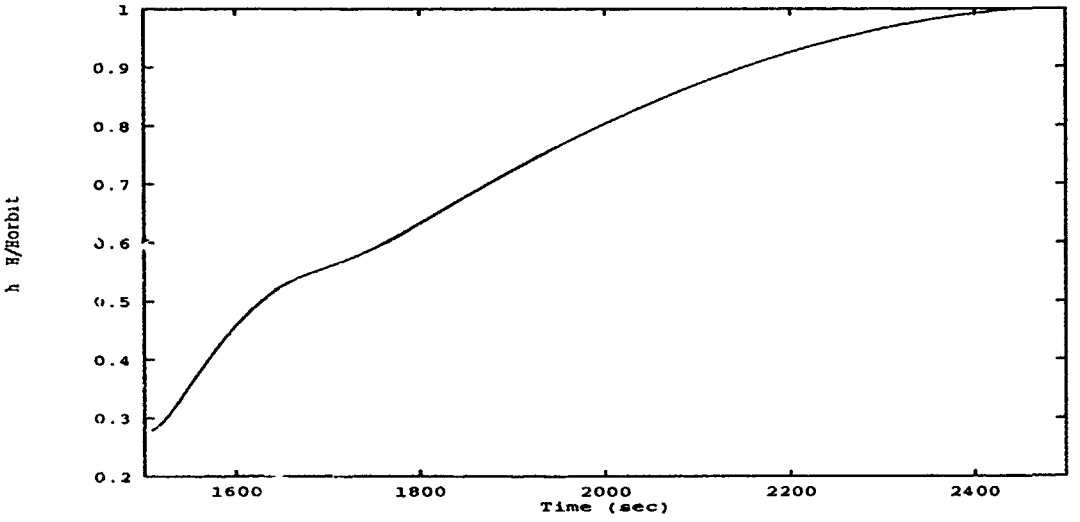

Figure 44. Suborbital Trajectory Altitude versus Time.

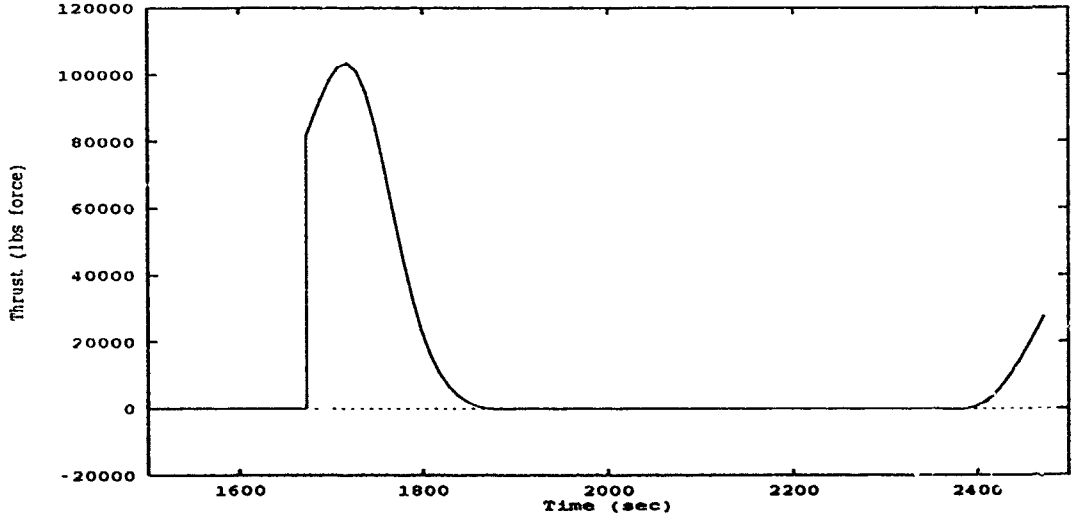

Figure 45. Suborbital Trajectory Thrust versus Time.

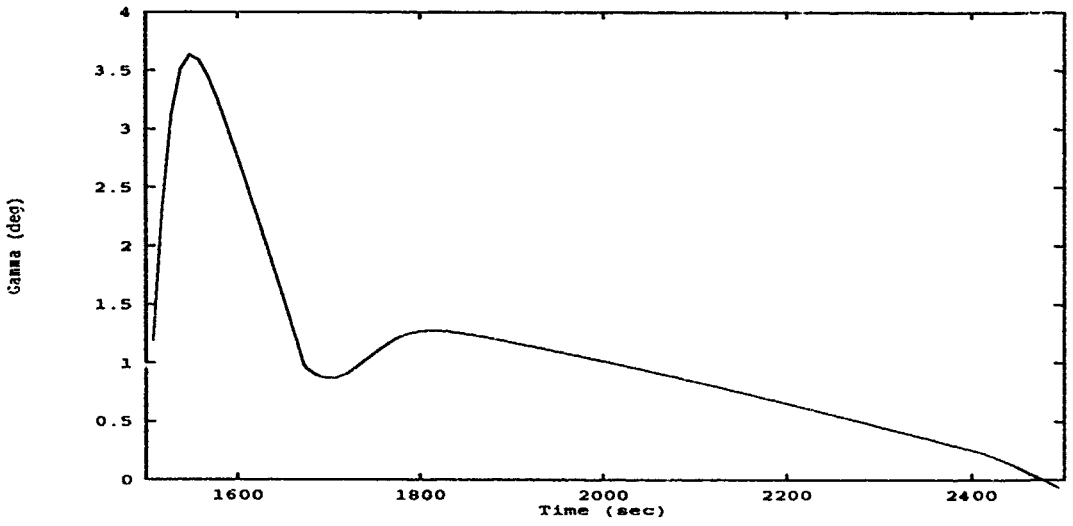

Figure 46. Suborbital Trajectory Flight Path Angle versus Time.

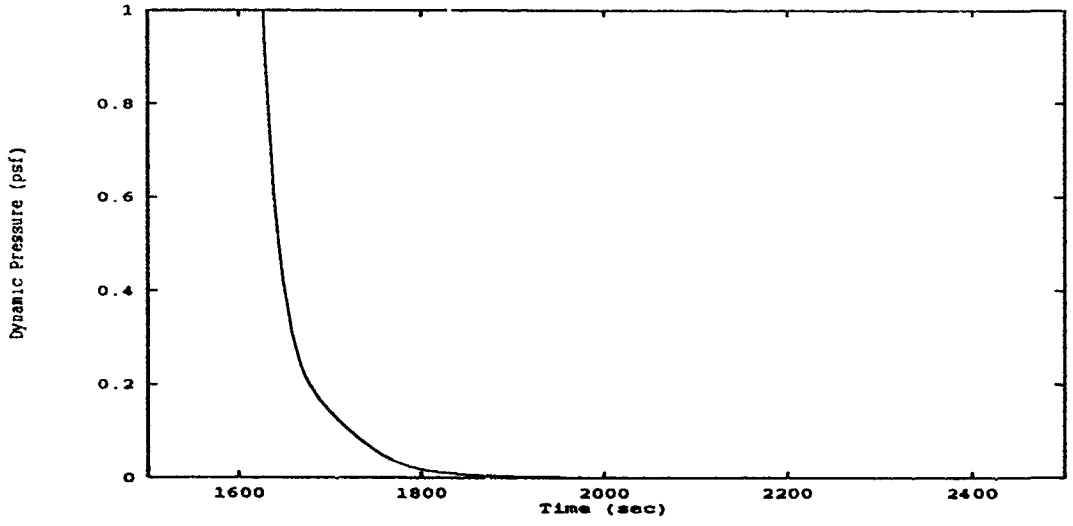

Figure 47. Suborbital Trajectory Dynamic Pressure versus Time.

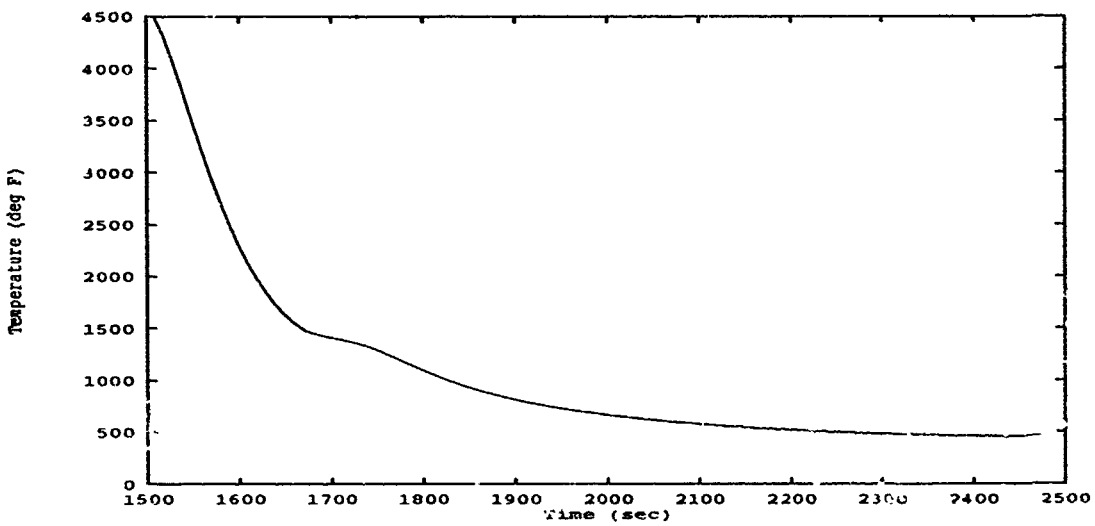

Figure 48. Suborbital Trajectory Temperature versus Time.

Bibliography

1. Anderson Jr, John D. *Hypersonic and High Temperature Gas Dynamics*. McGraw Hill, 1989.
2. Berarducci, M. "Navigation Sensor Shock Analysis Contract." McDonnell Douglas Technical Coordination Memo, June 1991.
3. Drummond, A. M. "Performance and Stability of Hypervelocity Aircraft Flying on a Minor Circle," *University of Toronto Institute for Aerospace Studies*, (135) (1968).
4. Gill, Philip E., et al. *Practical Optimization*. Academic Press, 1981
5. Hargraves, C. R. and S. W. Paris. "Direct Trajectory Optimization Using Nonlinear Programming and Collocation," *Journal of Guidance, Control, and Dynamics*, *10* (July-August 1987).
6. Kasten, Terry D. Personal Instruction on NASP Performance, October 1991.
7. Kasten, Terry D. "A National Utility Review," *SAE*, (911170) (1991).
8. Kauffman, H.G., et al. "Improved Airbreathing Launch Vehicle Performance with the use of Rocket Propulsion." Submitted for publication in Jounal of Spacecraft and Rockets.
9. Kors, D. "Design Considerations for Combined Air Breathing-Rocket Propulsion Systems," *AIAA*, (90-5216) (1990).
10. Lepsch Jr, Roger A. and others. "Utilizing Air-Turborocket and Rocket Propulsion for a Single-Stage-to-Orbit Vehicle," *AIAA*, (90-0295) (1990).
11. Martens, P. J., et al. *Optimal Trajectories by Implicit Simulation, Applications Manual*. Boeing Aerospace and Electronics, 1990.
12. Ravindran, A., et al. *Operations Research Principles and Practice*. John Wiley and Sons, 1987.
13. Salkeld, Robert. "Single-Stage Shuttles for Ground Launch and Air Launch." *Astronautics & Aeronautics*, 52–54 (March 1974).
14. Sponable, M. "Two Stage or Not to Stage," *AIAA*, (90-3835) (1990).
15. Sutton, George P. *Rocket Propulsion Elements*. John Wiley & Sons, 1986.
16. Vinh, Nguyen X. *Optimal Trajectories in Atmospheric Flight*. Elsevier Scientific Publishing Company, 1981.
17. Vlases, W. G., et al. *Optimal Trajectories by Implicit Simulation, Users Manual*. Boeing Aerospace and Electronics, 1990.

Vita

Capt. Mark R. Goodell graduated from Brigham Young University in 1986 with a Bachelor of Science Degree in Mechanical Engineering. Upon receiving an Air Force commission, he was assigned to Shemya AFB, AK where he served as a Crew Commander for the operation of the Cobra Dane radar system. Other duty assignments include Staff Officer at HQ AFSPACECOM/DOJ Peterson AFB, CO and Crew Commander at the 73rd Space Surveillance Squadron Falcon AFB, CO. Capt. Goodell was assigned to the Air Force Institute of Technology in May 1990.

Capt. Goodell is married to the forme Sechrest and has three children: Tinae, Shanell, and Skyler.

Permanent address: 656 Sykes Dr.
Idaho Falls, Idaho 83401

REPORT DOCUMENTATION PAGE

Form Approved
OMB No 0704-0188

Public report ng burden for th s collection of information is estimated to average 1 hour per response including the time for reviewing instruct ons searching existing data sources gathering and maintaining the data needed and completing and reviewing the collection of information Send comments rega ding this burden estimate or any other aspect of this collection of information including suggest ons for reducing this burden to Washington Headquarters Services, Directorate fo r nformation Operations and Reports, 1215 Jefferson Davis Highway, Suite 1204 Arlington, 2 2202-4302 and to the Office of Management and Budget Paperwork Reduction Proj ct (0704-0188) Washington DC 20503

1. AGENCY USE ONLY (Leave blank)	2. REPORT DATE	3. REPORT TYPE AND DATES COVERED
	December 1991	Master's Thesis

4. TITLE AND SUBTITLE

ANALYSIS OF SUBORBITAL LAUNCH TRAJECTORIES FOR SATELLITE DELI ERY

5. FUNDING NUMBERS

6. AUTHOR(S)

Mark R. Goodell, Captain, USAF

7. PERFORMING ORGANIZATION NAME(S) AND ADDRESS(ES)

Air Force Institute of Technology (AU)
Wright Patterson AFB, OH 45433-5000

8. PERFORMING ORGANIZATION REPORT NUMBER

AFIT/GA/ENY/91D-8

9. SPONSORING / MONITORING AGENCY NAME(S) AND ADDRESS(ES)

Terry D. Kasten
ASD/NAR
Wright Patterson AFB, OH 45433-5000

10. SPONSORING / MONITORING AGENCY REPORT NUMBER

11. SUPPLEMENTARY NOTES

12a. DISTRIBUTION / AVAILABILITY STATEMENT

Approved for public release; distribution unlimited

12b. DISTRIBUTION CODE

13. ABSTRACT *(Maximum 200 words)*

A computer simulation program was used to analyse performance of suborbital launch trajectories using a hypersonic NASP derived vehicle for satellite deployment. The trajectory investigated for this project involved satellite deployment at suborbital speeds. To deploy a satellite in this manner, a booster motor is used to insert the payload into orbit while the launch vehicle reenters and returns to earth. A simplified energy analysis was also formulated and used to determine the sensitivity of suborbital trajectory performance to specific design parameters. Results show that suborbital launch trajectories can increase the useful payload to orbit capacity over an identical vehicle flying a "typical" ascent where both the launch vehicle and payload are inserted into orbit. The amount of time available for payload deployment from a suborbital trajectory was also investigated with results showing that time periods on the order of ten minutes could be used for payload deployment.

14. SUBJECT TERMS	15. NUMBER OF PAGES
Suborbital Trajectories, Hypersonic Vehicles, Launch Vehicles	102
	16. PRICE CODE

17. SECURITY CLASSIFICATION OF REPORT	18. SECURITY CLASSIFICATION OF THIS PAGE	19. SECURITY CLASSIFICATION OF ABSTRACT	20. LIMITATION OF ABSTRACT
Unclassified	Unclassified	Unclassified	UL